Hacettepe Journal of Mathematics & Statistics

Hacet. J. Math. Stat.
Volume 51 (3) (2022), 857 – 881
DOI : 10.15672/hujms.1015660

Research Article

# A versatile family of generalized log-logistic distributions: bimodality, regression, and applications

Ahmad Alzaghal*[1], Mahmoud Aldeni[2]

[1] *The State University of New York at FSC, Farmingdale, NY 11735*
[2] *Western Carolina University, Cullowhee, NC 28723*

## Abstract

In real-world applications, it is not uncommon to encounter situations in which a set of data exhibits asymmetry and bimodality. Because of this, this paper proposes a new versatile family of generalized log-logistic distributions using the method of $T$-$R\{Y\}$ framework. The resulting flexible classes of this family includes both unimodal and bimodal distributions which can be expected to model a wide variety of data with different levels of skewness. The distributional and structural properties of the classes are discussed. The method of maximum likelihood is used for estimating the distributions parameters and a simulation study is conducted to examine its performance. The usefulness and goodness-of-fit of some members of these classes are illustrated by means of six real data sets. The strength of these members is shown consistently by giving better fits than some of the competitors with the same number of parameters. In addition, a new generalized log-logistic lifetime regression model is introduced and applied to fit a right-censored data with covariates. The flexibility provided by this model could be very helpful in describing and explaining different types of lifetime data.

**Mathematics Subject Classification (2020).** 60E05, 62E10, 62N01

**Keywords.** bimodal distributions, $T$-$R\{Y\}$ framework, lifetime regression model

## 1. Introduction

Over the last two decades, there has been a growing body of research that focused primarily on generalizing or modifying some well-known univariate distributions, and the research in this area continues to be quite active. The Beta-generated family [12] and the $T$-$R\{Y\}$ framework [2] are examples of such generalized families of distributions. In fact, researchers continue to build and develop new statistical distributions in order to get more flexibility and increase the accuracy in data modeling. Although adding one or more extra parameters to the baseline distributions may allow the new distributions to have different shapes, but in most cases these generalized distributions can only exhibit unimodal shapes. In real-world applications, there are situations in which the underlying distribution of a random variable follows bimodal probability distribution. For instance,

*Corresponding Author.
Email addresses: ahmad.alzaghal@farmingdale.edu (A. Alzaghal), maldeni@wcu.edu (M. Aldeni)
Received: 27.10.2021; Accepted: 21.02.2022

the natural log-transformed of the asteroid and echinoid egg size [11], the waiting time between eruptions and duration of eruptions of certain geysers [6, 15], the size of Weaver ant workers [20, 22], and the color of galaxies [7] are examples of such variables with bimodal distributions. All of these examples, as well as many others, demonstrate why it is advantageous for researchers to build new novel distributions capable of modeling a variety of forms, including skew-symmetric unimodal and bimodal shapes.

There are several research articles in the literature that presented and discussed different families of skew-symmetric bimodal distributions. For example, Sarma at al. [17] proposed a family of symmetric bimodal distributions, which is different from the mixture of two normal distributions. Another alternative to the two component normal mixtures, Hassan and Hijazi [16] considered the symmetric bimodal exponential power distribution.

The symmetry property of the aforementioned distributions can be considered a desirable feature in fitting symmetric data, but a limitation in modeling asymmetric data sets. For this reason, several extensions and generalizations are proposed in the literature to address this limitation, which can be used in data modeling in various real-world settings. For example, Azzalini and Bowman [6] introduced a family of skew-normal distributions and some extensions of this family to skew-symmetric unimodal and bimodal distributions can be found in [5, 14, 19], and others. In addition, different construction methods have been presented by many researchers that may allow generating skew-symmetric unimodal and bimodal distributions. For instance, Famoye et al. [13] studied the bimodality properties of the beta-normal distribution, which was constructed using the beta-generated family of distributions [12]. Al-Aqtash et al. [1], for example, used the $T$-$X$ family of distributions [3] to generate the Gumbel-Weibull distribution and study its regions of unimodality and bimodality. Moreover, Alzaatreh [4] proposed the bimodal Weibull-Gamma {log-logistic} distribution using the $T$-$R\{Y\}$ framework (see [2]).

The $T$-$R\{Y\}$ framework [2] is defined as follows: Let $T$, $R$ and $Y$ be random variables with cumulative distribution functions (CDFs) $F_T$, $F_R$, and $F_Y$, respectively, and the corresponding quantile functions $Q_T$, $Q_R$ and $Q_Y$. The probability density functions (PDFs) (if they exist) will be denoted by $f_T$, $f_R$, and $f_Y$, respectively. Then the CDF and the PDF of the random variable $X = Q_R\left(F_Y(T)\right)$ are given, respectively, by

$$F_X(x) = \int_a^{Q_Y(F_R(x))} f_T(t)dt = F_T\left(Q_Y\left(F_R(x)\right)\right), \tag{1.1}$$

where $T, Y \in [a, b]$, for $-\infty \leq a < b \leq \infty$, and

$$f_X(x) = f_R(x) \times \frac{f_T\left(Q_Y\left(F_R(x)\right)\right)}{f_Y\left(Q_Y\left(F_R(x)\right)\right)}. \tag{1.2}$$

The $T$-$R\{Y\}$ framework is a desirable method for developing new versatile and wide classes and families of generalized distributions for any given random variable $R$. In this paper, we assume the random variable $R$ follows the log-logistic distribution. The log-logistic distribution is one of the important continuous distributions defined by one shape and one scale parameters. It is used in survival analysis, hydrology, economy, and different fields of study. In addition to the closed form of its CDF, the log-logistic model can have monotonic and non-monotonic (hump-shaped) hazard rate function, which is useful in lifetime data analysis with censoring.

The motivation of this paper is to introduce a new family of unimodal and bimodal skew-symmetric distributions that generalizes or extends the log-logistic distribution. Focusing on modeling real-world data sets, this article aims to present flexible members of this family that are able to model unimodal and bimodal shapes with different degrees of skewness and provide a better fit than some distributions in the literature with the same or more numbers of parameters. Moreover, unlike many other generalized distributions, the closed form expressions for their CDFs make it much easier to simulate random samples from these distributions or to carry out quantile regressions.

The rest of this article is outlined as follows. Section 2 defines the $T$-Log-Logistic$\{Y\}$ family of generalized log-logistic distributions and derives classes of this family using the quantile functions of exponential, logistic, and Cauchy distributions. Some structural properties of the proposed families are investigated in Section 3. Some new members of these families are studied in Section 4. In Section 5, we address parameter estimation and simulation for the Normal-log-logistic-Cauchy distribution using the Maximum Likelihood (ML) method. The usefulness of the new proposed family of distributions is illustrated through six applications to real data sets in Section 6. In Section 7, a new generalized log-logistic regression model is introduced and applied to a right censored lifetime data set. Lastly, Section 8 summarizes the main findings and concludes the article.

## 2. The family and classes of generalized log-logistic distribution

In this section, firstly, we define the $T$-log-logistic$\{Y\}$ ($T$-$LL\{Y\}$) family of generalized log-logistic distribution. Let $R$ be a random variable that follows the log-logistic distribution, then the CDF and PDF are, respectively, given by

$$F_R(x) = \frac{1}{1 + (x/\beta)^{-\alpha}} \tag{2.1}$$

and

$$f_R(x) = \frac{\alpha}{\beta}\frac{(x/\beta)^{\alpha-1}}{(1 + (x/\beta)^{\alpha})^2}. \tag{2.2}$$

The definition in Equation (1.1) gives the CDF of the random variable $X$ in $T$-$LL\{Y\}$ families of distributions as

$$F_X(x) = \int_a^{Q_Y\left[\left(1+(x/\beta)^{-\alpha}\right)^{-1}\right]} f_T(t)dt = F_T\left(Q_Y\left[\left(1 + (x/\beta)^{-\alpha}\right)^{-1}\right]\right), \tag{2.3}$$

and the corresponding PDF associated with Equation (2.3) is

$$f_X(x) = \frac{(\alpha/\beta)(x/\beta)^{\alpha-1}}{(1 + (x/\beta)^{\alpha})^2}\frac{f_T\left(Q_Y\left[\left(1 + (x/\beta)^{-\alpha}\right)^{-1}\right]\right)}{f_Y\left(Q_Y\left[\left(1 + (x/\beta)^{-\alpha}\right)^{-1}\right]\right)}. \tag{2.4}$$

Secondly, we define three generalized $T$-$LL\{Y\}$ classes of distributions based on the quantile functions of exponential, logistic, and Cauchy distributions defined in Table 1.

**Table 1.** Some quantile functions of $Y$ and the domains of $T$.

| | Random variable $Y$ | The quantile function $Q_Y(p)$ | Domain of $T$ |
|---|---|---|---|
| (i) | Exponential | $-\log[1-p]$ | $(0,\infty)$ |
| (ii) | Logistic | $\log[p/(1-p)]$ | $(-\infty,\infty)$ |
| (iii) | Cauchy | $\tan(\pi[p-0.5])$ | $(-\infty,\infty)$ |

The following are some classes of generalized log-logistic distributions:

### 2.1. The *T*-log-logistic{exponential} class of distributions

By using the quantile function of the exponential distribution in Table 1, the CDF of the $T$-log-logistic{exponential} ($T$-$LL\{E\}$) class of distributions using Equation (2.3) is given by

$$F_X(x) = F_T\left\{-\log\left[1 - (1 + (x/\beta)^{-\alpha})^{-1}\right]\right\}, \tag{2.5}$$

and the corresponding PDF to Equation (2.5) using Equation (2.4) is

$$f_X(x) = \frac{(\alpha/\beta)(x/\beta)^{\alpha-1}}{1+(x/\beta)^{\alpha}} f_T \left\{ -\log \left[ 1 - (1+(x/\beta)^{-\alpha})^{-1} \right] \right\}. \tag{2.6}$$

Note that the $T$-$LL\{E\}$ class of distributions arises from the hazard function of the log-logistic distribution. In fact, the CDF and PDF of the $T$-$LL\{E\}$ class of distributions can be written as $F_X(x) = F_T\{H_R(x)\}$ and $f_X(x) = h_R(x) f_T\{H_R(x)\}$, where $h_R(x)$ and $H_R(x)$ are the hazard and cumulative hazard functions of the log-logistic distribution, respectively.

### 2.2. The *T*-log-logistic{logistic} class of distributions

By using the quantile function of the logistic distribution in Table 1, the CDF of the $T$-log-logistic{logistic} ($T$-$LL\{L\}$) class of distributions using Equation (2.3) is given by

$$F_X(x) = F_T \left\{ \log \left( \frac{(1+(x/\beta)^{-\alpha})^{-1}}{1-(1+(x/\beta)^{-\alpha})^{-1}} \right) \right\} = F_T \left\{ \log\left(x/\beta\right)^{\alpha} \right\}, \tag{2.7}$$

and the corresponding PDF to Equation (2.7) using Equation (2.4) is

$$f_X(x) = \frac{\alpha}{x} f_T \left\{ \log \left( \frac{(1+(x/\beta)^{-\alpha})^{-1}}{1-(1+(x/\beta)^{-\alpha})^{-1}} \right) \right\} = \frac{\alpha}{x} f_T \left\{ \log\left(x/\beta\right)^{\alpha} \right\}. \tag{2.8}$$

Note that the $T$-$LL\{L\}$ class of distributions is considered a class arising from the logit function of the log-logistic distribution.

### 2.3. The *T*-log-logistic{Cauchy} class of distributions

By using the quantile function of the Cauchy distribution in Table 1, the CDF of the $T$-log-logistic{Cauchy} ($T$-$LL\{C\}$) class of distributions using Equation (2.3) is given by

$$F_X(x) = F_T\left\{\tan(u)\right\}, \tag{2.9}$$

and the corresponding PDF to Equation (2.9) using Equation (2.4) is

$$f_X(x) = \frac{(\pi\alpha/\beta)(x/\beta)^{\alpha-1}}{(1+(x/\beta)^{\alpha})^2} \sec^2(u)\, f_T\left\{\tan(u)\right\}, \tag{2.10}$$

where $u = \pi[(1+(x/\beta)^{-\alpha})^{-1} - 0.5]$.

## 3. Some distributional and structural properties

In this section, we highlight some of the general properties of the $T$-$LL\{Y\}$ classes of distributions, including transformations, quantile functions, implicit formula for the mode(s), Shannons entropies, moments and mean deviations.

**Theorem 3.1** (Transformation)**.** *Let $Q_R(\cdot)$ be the quantile function of the random variable $R$, then the random variable $X = Q_R(F_Y(T))$ follows the $T$-$R\{Y\}$ family of distributions. In particular, if the random variable $R$ follows the log-logistic distribution, then the random variable $X = \beta\left(\frac{1-F_Y(T)}{F_Y(T)}\right)^{-1/\alpha}$ follows the $T$-$LL\{Y\}$ family of distributions.*

***Proof.*** The CDF $F_X(x) = F_T(Q_Y(F_R(x)))$ in Equation (1.1), where $T = Q_Y(F_R(X))$, implies $X = Q_R(F_Y(T))$. The second result follows directly from using the transformation $X = Q_R(F_Y(T))$, where $Q_R(p) = \beta\left(\frac{1-p}{p}\right)^{-1/\alpha}$ is the quantile function of log-logistic distribution. □

**Remark 3.2.** Theorem 3.1 can be used to generate a random sample from the random variable $X$ when a random variable $T$ and the quantile function of a random variable $Y$ are specified.

**Corollary 3.3.** *Using Theorem 3.1, the random variable*

i. $X = \beta\left(1 - e^{-T}\right)^{1/\alpha}$ *follows the T-LL{E} distribution.*
ii. $X = \beta e^{T/\alpha}$ *follows the T-LL{L} distribution.*
iii. $X = \beta\left(\frac{1/2-\pi\arctan(T)}{1/2+\pi\arctan(T)}\right)^{-1/\alpha}$ *follows the T-LL{C} distribution.*

**Theorem 3.4** (Quantiles)**.** *Let $Q_X(p)$, $0 < p < 1$, denote the quantile function of the random variable $X$. Then, the quantile function for the T-R{Y} family of distributions is given by*

$$Q_X(p) = Q_R\left\{F_Y(Q_T(p)\right\}.$$

*In particular, if the random variable R follows the log-logistic distribution, then the quantile function for the T-LL{Y} family of distributions is given by*

$$Q_X(p) = \beta\left(\frac{1 - F_Y(Q_T(p))}{F_Y(Q_T(p))}\right)^{-1/\alpha}.$$

***Proof.*** The results follow directly by using the relation $F_X(x) = F_T\left(Q_Y\left(F_R(x)\right)\right)$, and then solving $F_X\left(Q_X\left(p\right)\right) = p$ for $Q_X\left(p\right)$. □

**Corollary 3.5.** *Using Theorem 3.4, the quantile functions for the (i) T-LL{E}, (ii) T-LL{L}, (iii) T-LL{C}, classes of distributions, respectively, are*

i. $Q_X(p) = \beta\left(1 - e^{-Q_T(p)}\right)^{1/\alpha}$,
ii. $Q_X(p) = \beta e^{Q_T(p)/\alpha}$,
iii. $Q_X(p) = \beta\left(\frac{1/2-\pi\arctan(Q_T(p))}{1/2+\pi\arctan(Q_T(p))}\right)^{-1/\alpha}$.

Note that the median can be also obtained by setting $p = 0.5$ in the quantile functions in Corollary 3.5.

**Theorem 3.6.** *The mode(s) of the T-LL{Y} family of distributions are the solutions of the equation*

$$\Psi\left\{f_T\left(Q_y\left(F_R(x)\right)\right)\right\} = \frac{1-\alpha}{x} - \frac{2\alpha\beta^{2\alpha-1}}{x^{2\alpha}}\left(1 + (x/\beta)^{-\alpha}\right)^{-1} + \Psi\left\{f_y\left(Q_y\left(F_R(x)\right)\right)\right\}, \quad (3.1)$$

*where $\Psi(f) = f'/f$.*

***Proof.*** The derivative of $f_R(x)$ is given by $f'_R(x) = f_R(x)\left(\frac{\alpha-1}{x} + \frac{2\alpha\beta^{2\alpha-1}}{x^{2\alpha}}\left(1 + (x/\beta)^{-\alpha}\right)^{-1}\right)$, which implies that the derivative of $f_X(x)$ can be written as $f'_X(x) = f_X(x)E(x)$ where $E(x) = \frac{\alpha-1}{x} + \frac{2\alpha\beta^{2\alpha-1}}{x^{2\alpha}}\left(1 + (x/\beta)^{-\alpha}\right)^{-1} + \Psi\left\{f_T\left(Q_y\left(F_R(x)\right)\right)\right\} - \Psi\left\{f_y\left(Q_y\left(F_R(x)\right)\right)\right\}$. By setting $E(x) = 0$ and solving for $x$ we obtain the mode(s) of $f_X(x)$, which are the solutions of the Equation (3.1). □

**Corollary 3.7.** *Using Theorem 3.6, the mode(s) of the (i) T-LL{E}, (ii) T-LL{L}, (iii) T-LL{C} distributions are solutions of the following equations, respectively,*

(i) $\Psi\left\{f_T\left(\log(1 + (x/\beta)^{\alpha})\right)\right\} = \frac{1-\alpha}{x} - \frac{2\alpha\beta^{2\alpha-1}}{x^{2\alpha}}\left(1 + (x/\beta)^{-\alpha}\right)^{-1} - \frac{\alpha}{x}\left(1 + (x/\beta)^{-\alpha}\right)^{-1}$,
(ii) $\Psi\left\{f_T\left(\alpha\log(x/\beta)\right)\right\} = \frac{1-\alpha}{x} - \frac{2\alpha\beta^{2\alpha-1}}{x^{2\alpha}}\left(1 + (x/\beta)^{-\alpha}\right)^{-1} + \frac{\alpha}{x}\left(\frac{1-(x/\beta)^{\alpha}}{1+(x/\beta)^{\alpha}}\right)$
(iii) $\Psi\left\{f_T\left(\tan\left(\pi\left[\frac{1}{1+(x/\beta)^{-\alpha}} - 0.5\right]\right)\right)\right\} = \frac{1-\alpha}{x} - \frac{2\alpha\beta^{2\alpha-1}}{x^{2\alpha}}\left(1 + (x/\beta)^{-\alpha}\right)^{-1} - \frac{2\alpha\pi}{x}\frac{(x/\beta)^{\alpha}}{(1+(x/\beta)^{\alpha})^2}\cot\left[\pi(1 + (x/\beta)^{\alpha})^{-1}\right]$.

**Remark 3.8.** The distributions in Subsections 4.3, 4.4, and 4.5 are examples of bimodal distributions. Thus, the equation in Corollary 3.7 (iii) could have more than one solution to represent a bimodal distribution.

The entropy of a random variable $X$ is a measure of variation of uncertainty. Entropy has several applications in engineering, information theory, chemistry, and physics. The Shannons entropy for a continuous random variable $X$ with PDF $f(x)$ is defined as $\eta_X = E[-\log f(x)]$ ([18]).

**Theorem 3.9.** *The Shannon's entropy for the T-LL{Y} family of distributions is given by*

$$\eta_X = \eta_T + E\left(\log f_Y(T)\right) + \log\left(\beta^\alpha/\alpha\right) + (1-\alpha)E\left(\log X\right) + 2E\left(\log\left(1+(X/\beta)^\alpha\right)\right),$$

*where, $\eta_T$ is the Shannon's entropy for the random variable $T$.*

***Proof.*** By the definition of Shannon's entropy,

$$\eta_X = E\left\{-\log f_T\left(Q_y\left\{F_R(X)\right\}\right)\right\} + E\left\{\log f_Y\left(Q_y\left\{F_R(X)\right\}\right)\right\} + E\left\{-\log f_R(X)\right\}.$$

Since the random variable $T$ can be written as $T = Q_y\left\{F_R(X)\right\}$, then $\eta_X$ can be reduced to

$$\eta_X = \eta_T + E\left(\log f_Y(T)\right) + E\left\{-\log(f_R(X))\right\}.$$

It can be shown that,

$$E\left\{-\log(f_R(X))\right\} = \log\left(\beta^\alpha/\alpha\right) + (1-\alpha)E\left(\log X\right) + 2E\left(\log\left(1+(X/\beta)^\alpha\right)\right).$$

Hence, $\eta_X = \eta_T + E\left(\log f_Y(T)\right) + \log\left(\beta^\alpha/\alpha\right) + (1-\alpha)E\left(\log X\right) + 2E\left(\log\left(1+(X/\beta)^\alpha\right)\right)$. □

**Corollary 3.10.** *Based on Theorem 3.9, the Shannon's entropies of the (i) T-LL{$E$}, (ii) T-LL{$L$}, (iii) T-LL{$C$} classes of distributions, respectively, are given by*

(i) $\eta_X = \eta_T - \mu_T + \log\left(\beta^\alpha/\alpha\right) + (1-\alpha)E\left(\log X\right) + 2E\left(\log\left(1+(X/\beta)^\alpha\right)\right),$

(ii) $\eta_X = \eta_T - \mu_T - 2E\left(\log(1+e^{-T})\right) + \log\left(\beta^\alpha/\alpha\right) + (1-\alpha)E\left(\log X\right) + 2E\left(\log\left(1+(X/\beta)^\alpha\right)\right),$

(iii) $\eta_X = \eta_T + E\left(-\log(1+e^{-T})\right) - \log\pi + \log\left(\beta^\alpha/\alpha\right) + (1-\alpha)E\left(\log X\right) + 2E\left(\log\left(1+(X/\beta)^\alpha\right)\right),$

*where $\mu_T$ is the mean for the random variable $T$.*

**Theorem 3.11.** *Let $X$ be a random variable that follows the T-LL{Y} family. Assume that $E(X^r) < \infty$ for all $r$, then*

$$E(X^r) \le \beta^r\, B\left(1-r/\alpha, 1+r/\alpha\right) E\left(\left\{\bar{F}_Y(T)\right\}^{-1}\right)$$

*whenever $\alpha > r$, where $\bar{F}_Y(T) = 1 - F_Y(T)$.*

***Proof.*** If $f_R(x)$ is the PDF of a non-negative random variable $R$, then the $r^{th}$ non-central moment of the random variable $T$-$R\{Y\}$ satisfies $E\left(X^r\right) \le E(R^r)E\left(\left\{\bar{F}_Y(T)\right\}^{-1}\right)$. (see Theorem 1, [2]). The results follows using the fact that the $r^{th}$ non-central moment of the log-logistic distribution with parameters $\alpha$ and $\beta$ is

$$E\left(R^r\right) = \beta^r B\left(1-r/\alpha, 1+r/\alpha\right),$$

where $B$ is the beta function given by $B(x,y) = \int_0^1 t^{x-1}(1-t)^{y-1}\,dt$. □

The following theorem provides the $r^{th}$ non-central moment for $T$-$LL\{Y\}$ family of distributions.

**Theorem 3.12.** *The $r^{th}$ non-central moments for the T-LL{Y} family of distributions are given by*

$$E(X^r) = \beta^r \sum_{k=0}^{\infty} w_k E[(F_Y(T))^{k+r/\alpha}],$$

*where $w_k = (-1)^k\binom{-r/\alpha}{k}$.*

***Proof.*** If $Q_R(\cdot)$ is the quantile function of a random variable $R$, then by using Theorem (3.1), $E(X^r) = E(Q_R(F_Y(T)))^r$. By applying the generalized binomial expansion, $(Q_R(p))^r$ can be written as $(Q_R(p))^r = \beta^r \sum_{k=0}^{\infty} w_k E\left[(F_y(T))^{k+r/\alpha}\right]$, where $w_k$ defined in the statement of Theorem 3.12, which in turn implies the result. □

**Corollary 3.13.** *Based on Theorem 3.12, the $r^{th}$ non-central moments for the (i) T-LL$\{E\}$, (ii) T-LL$\{L\}$, (iii) T-LL$\{C\}$ classes of distributions, respectively, are*

(i) $E(X^r) = \beta^r \sum_{k=0}^{\infty} w_k \sum_{n=0}^{\infty} \binom{k+r/\alpha}{n} (-1)^n M_T(-n)$, *exists if* $M_T(-n) < \infty$,

(ii) $E(X^r) = \beta^r \sum_{k=0}^{\infty} w_k \sum_{n=0}^{\infty} \binom{-(k+r/\alpha)}{n} M_T(-n)$, *exists if* $M_T(-n) < \infty$,

(iii) $E(X^r) = \beta^r \sum_{k=0}^{\infty} w_k \sum_{n=0}^{\infty} \binom{k+r/\alpha}{n} (2)^{n-(k+r/\alpha)} \pi^{-n} E(\arctan T)^n$, *exists if* $E(\arctan T)^n < \infty$,

*where* $M_X(t) = E(e^{tX})$.

Expressions of statistical measures such as the mean, variance, skewness, and kurtosis can be derived from Corollary 3.13. The following theorem provides the mean deviation from the mean, $D(\mu)$, and the mean deviation from the median, $D(M)$, for the *T-LL*$\{Y\}$ family of distributions.

**Theorem 3.14.** *The $D(\mu)$ and $D(M)$ for the T-LL$\{Y\}$ family of distributions, respectively, are given by*

$$D_\mu = 2\mu F_T(Q_Y(F_R(\mu))) - 2I_\mu, \text{ and } D_M = \mu - 2I_M,$$

*where $\mu$ and $M$ are the mean and median for $X$, and*

$$I_q = \beta \sum_{n=0}^{\infty} w_n \int_{Q_Y(F_R(0))}^{Q_Y(F_R(q))} f_T(u) F_Y^{n+1/\alpha}(u)\, du,$$

*where* $w_n = \binom{-\alpha^{-1}}{n}(-1)^n$.

***Proof.*** The mean deviation from the mean and the mean deviation from the median for a nonnegative random variable $X$ are given by, respectively, $D_\mu = E(|X-\mu|) = 2\mu F_X(\mu) - 2I_\mu$, and $D_M = E(|X-M|) = \mu - 2I_M$, where $I_q = \int_0^q x f_X(x)\, dx$. From Equation (1.2) and Theorem 3.4, we have $I_q = \int_{Q_Y(F_R(0))}^{Q_Y(F_R(q))} f_T(u)\, Q_R(F_Y(u))\, du$. By using the series expansion of $Q_R(\cdot)$, we obtain the result in Theorem 3.14 □

**Corollary 3.15.** *Based on Theorem 3.14, the $I(q)$s for (i) T-LL$\{E\}$, (ii) T-LL$\{L\}$, (iii) T-LL$\{C\}$ classes of distributions, respectively, when $S_\xi(q,z,r) = \int_z^{Q_Y(F_R(q))} \xi^r f_T(u) du$, are given by*

(i) $I_q = \beta \sum_{n=0}^{\infty} \sum_{m=0}^{\infty} w_n \binom{n+1/\alpha}{m} (-1)^m S_{e^{-u}}(q,0,m)$, *where $Q_Y$ for exponential distribution.*

(ii) $I_q = \beta \sum_{n=0}^{\infty} \sum_{m=0}^{\infty} w_n \binom{-(n+1/\alpha)}{m} (-1)^m S_{e^{-u}}(q,-\infty,m)$, *where $Q_Y$ for logistic distribution.*

(iii) $I_q = \beta \sum_{n=0}^{\infty} \sum_{m=0}^{\infty} w_n \binom{n+1/\alpha}{m} (1/2)^{n+1/\alpha-m} S_{\pi^{-1}\arctan(u)}(q,-\infty,m)$, *where $Q_Y$ for Cauchy distribution.*

Theorem 3.14 and Corollary 3.15 can be used to obtain the mean deviations for the *T-LL*$\{E\}$, *T-LL*$\{L\}$, and *T-LL*$\{C\}$ classes of distributions.

## 4. Some new generalized log-logistic distributions

In this section, different $T$ and $Y$ distributions are used to generate flexible members of the *T-LL*$\{Y\}$ family of distributions. We present five new *T-LL*$\{Y\}$ distributions namely, Weibull-*LL*$\{$exponential$\}$, exponentiated-exponential-*LL*$\{$exponential$\}$, logistic-*LL*$\{$Cauchy$\}$, Gumbel-*LL*$\{$Cauchy$\}$, and normal-*LL*$\{$Cauchy$\}$.

### 4.1. The Weibull-log-logistic{exponential} distribution

If the random variable $T$ follows the Weibull distribution with parameters $\mu$ (shape) and $\sigma$ (scale), then the CDF of the random variable $T$ is $F_T(x) = 1 - e^{-(x/\sigma)^{\mu}}$, where $x \geq 0$ and $\sigma, \mu > 0$. Using Equation (2.5), the CDF of the Weibull-log-logistic-{exponential} (*W-LL{E}*) distribution is defined as

$$f_X(x) = F_X(x) = 1 - e^{-((1/\sigma)\log[1+(x/\beta)^{\alpha}])^{\mu}}, \tag{4.1}$$

and the corresponding PDF using Equation (2.6) is given by

$$f_X(x) = \frac{(\alpha\mu/\beta)(x/\beta)^{\alpha-1}}{\sigma^{\mu}\left(1+(x/\beta)^{\alpha}\right)} \left(\log\left[1+(x/\beta)^{\alpha}\right]\right)^{\mu-1} e^{-((1/\sigma)\log[1+(x/\beta)^{\alpha}])^{\mu}},$$

where $x > 0$ and $\alpha, \beta, \sigma, \mu > 0$.

When $\mu = 1$, the *W-LL{E}* distribution reduces to the Burr Type XII distribution, and when $\mu = \alpha = 1$, the *W-LL{E}* distribution becomes the Pareto Type II (Lomax) distribution. Figure 1 provides graphs of the PDF of *W-LL*{*E*} for various values of $\alpha, \beta, \sigma$, and $\mu$. These graphs show that the *W-LL*{*E*} distribution can be skewed to right, skewed to the left, symmetric, or have a reversed J-shape.

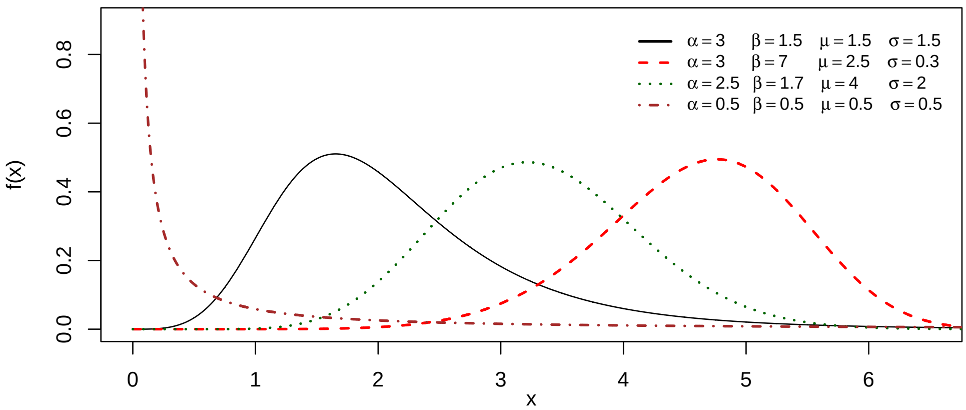


**Figure 1.** The PDFs of *W-LL*{*E*} for various parameter values.

Some of the general properties of *W-LL*{*E*} distribution can be obtained by using the general properties of the *T-LL*{*Y*} family of distributions derived in Section 3.

(i) Quantile function: By using Corollary 3.5 part (i), the quantile function of the *W-LL*{*E*} distribution is given by

$$Q_X(p) = \beta\left(1 - e^{-\sigma(-\log(1-p))^{1/\mu}}\right)^{1/\alpha}.$$

(ii) Mode: By using Corollary 3.7 part (i), the unique mode of *W-LL*{*E*} distribution is the solution of the following equation

$$\frac{\alpha(x/\beta)^{\alpha}}{x\left(1+(x/\beta)^{\alpha}\right)} \frac{\left(1+\mu\left\{-1+\left(\sigma^{-1}\log\left[1+(x/\beta)^{\alpha}\right]\right)^{\mu}\right\}\right)}{\log\left[1+(x/\beta)^{\alpha}\right]}$$

$$= \frac{\alpha-1}{x} + \frac{2\alpha\beta^{2\alpha-1}}{x^{2\alpha}}\left(1+(x/\beta)^{-\alpha}\right)^{-1} + \frac{\alpha}{x}\left(1+(x/\beta)^{-\alpha}\right)^{-1},$$

which can be evaluated numerically.

(iii) Shannons entropy: By using Corollary 3.10 part (i), the Shannons entropy of *W-LL*{*E*} distribution is given by

$$\eta_X = \sigma(1-1/\mu) + \ln(\sigma/\mu) + 1 - \sigma\Gamma(1+1/\mu) + \log\left(\beta^{\alpha}/\alpha\right)$$
$$+(1-\alpha)E\left(\log X\right) + 2E\left(\log\left(1+(X/\beta)^{\alpha}\right)\right).$$

(iv) Moments: By using Corollary 3.13 part (i), the $r^{th}$ non-central moments of *W-LL*$\{E\}$ distribution are given by

$$E(X^r) = \beta^r \sum_{k=0}^{\infty} w_k \sum_{n,m=0}^{\infty} \binom{k+r/\alpha}{n} (-1)^n \frac{(-n)^m \sigma^m}{m!} \Gamma(1+m/\mu),$$

where $w_k = (-1)^k \binom{-r/\alpha}{n}$.

(v) Mean deviations: By using Corollary 3.15 part (i), the $D_\mu$ and the $D_M$ of *W-LL*$\{E\}$ distribution are given by

$$D_\mu = 2\mu F_T(Q_Y(F_R(\mu))) - 2I_\mu, \text{and } D_M = \mu - 2I_M,$$

where $I_q$ is given by

$$I_q = \beta\mu \sum_{n,m,k=0}^{\infty} w_h \int_0^{(q/\sigma)^\mu} (u/\sigma)^{\mu-1} e^{-(u/\sigma)^\mu + ku},$$

and $w_h = \binom{-\alpha^{-1}}{n}\binom{n+1/\alpha}{m}\binom{n+1/\alpha}{k}(-1)^{n+m+k}$.

### 4.2. The exponentiated-exponential-log-logistic{exponential} distribution

If the random variable $T$ follows the exponentiated-exponential distribution with parameters $\mu$ (shape) and $\sigma$ (scale), then the CDF of the random variable $T$ is $F_T(x) = (1 - e^{-(x/\sigma)})^\mu$, where $x \geq 0$ and $\sigma, \mu > 0$. Using Equation (2.5), the CDF of the exponentiated exponential-log-logistic-{exponential} (*EE-LL*$\{E\}$) distribution is defined as

$$F_X(x) = \left(1 - \left(1 - (1 + (x/\beta)^{-\alpha})^{-1}\right)^{\frac{1}{\sigma}}\right)^\mu,$$

and the corresponding PDF using Equation (2.6) is given by

$$f_X(x) = \tfrac{(\alpha\mu/\beta\sigma)(x/\beta)^{\alpha-1}}{(1+(x/\beta)^\alpha)^2} \left(1 - (1 + (x/\beta)^{-\alpha})^{-1}\right)^{\frac{1}{\sigma}-1} \left(1 - \left(1 - (1 + (x/\beta)^{-\alpha})^{-1}\right)^{\frac{1}{\sigma}}\right)^{\mu-1},$$

where $x > 0$ and $\alpha, \beta, \sigma, \mu > 0$.

Similar to the *W-LL*$\{E\}$, the *EE-LL*$\{E\}$ distribution reduces to the Burr Type XII distribution when $\mu = 1$, and when $\mu = \alpha = 1$, the *EE-LL*$\{E\}$ distribution becomes the Pareto Type II (Lomax) distribution. In Figure 2, various plots of the *EE-LL*$\{E\}$ are provided for different values of the parameters $\alpha, \beta, \sigma$, and $\mu$. The graphs show that the *EE-LL*$\{E\}$ distribution can be skewed to right, skewed to the left, symmetric, or have a reversed J-shape.

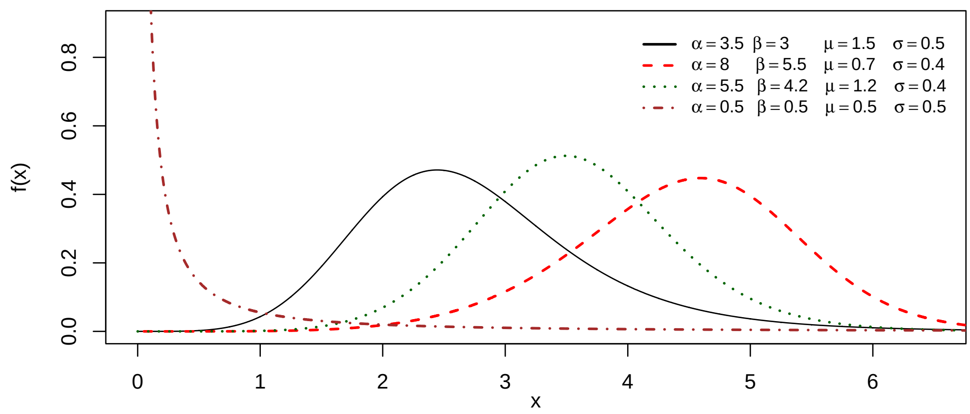


**Figure 2.** The PDFs of *EE-LL*$\{E\}$ for various parameter values.

### 4.3. The logistic-log-logistic{Cauchy} distribution

If the random variable $T$ follows the logistic distribution with parameters $\mu$ (shape) and $\sigma$ (scale), then the CDF of the random variable $T$ is $F_T(x) = \left(1 - e^{-(x-\mu)/\sigma}\right)^{-1}$, where $-\infty < x, \mu < \infty$ and $\sigma > 0$. Using Equation (2.9), the CDF of the logistic-log-logistic{Cauchy}($L$-$LL\{C\}$) distribution is defined as

$$F_X(x) = \left(1 - e^{-(\tan(u)-\mu)/\sigma}\right)^{-1},$$

and the corresponding PDF using Equation (2.10) is given by

$$f_X(x) = \frac{(\pi\alpha/\beta\sigma)(x/\beta)^{\alpha-1}}{(1+(x/\beta)^{\alpha})^2} \sec^2(u) \frac{e^{-(\{\tan(u)\}-\mu)/\sigma}}{\left(1 - e^{-(\{\tan(u)\}-\mu)/\sigma}\right)^2},$$

where $u = \pi[(1+(x/\beta)^{-\alpha})^{-1} - 0.5]$, $x > 0$, $\beta, \sigma > 0$, and $-\infty < \alpha, \mu < \infty$.

Figure 3 provides graphs of the PDF of $L$-$LL\{C\}$ for various values of $\alpha, \beta, \sigma$, and $\mu$. These graphs indicate that the $L$-$LL\{C\}$ distribution can be monotonically decreasing (reversed J-shape) with one mode at $x = 0$. It can be also symmetric, right skewed, or left skewed with one mode at $x > 0$, or bimodal with two different modes at $x_1, x_2 > 0$.

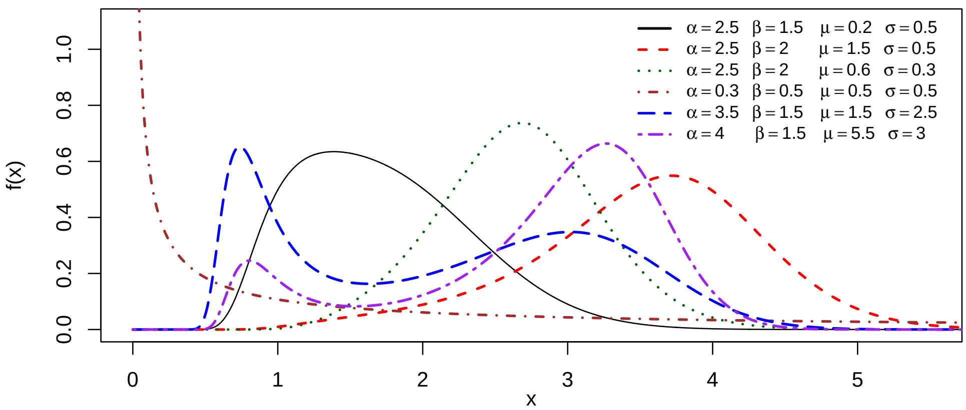


**Figure 3.** The PDFs of $L$-$LL\{C\}$ for various parameter values.

### 4.4. The Gumbel-log-logistic{Cauchy} distribution

If the random variable $T$ follows the Gumbel distribution with parameters $\mu$ (Shape) and $\sigma$ (Scale), then the CDF of the random variable $T$ is $F_T(x) = e^{-e^{-(x-\mu)/\sigma}}$, where $-\infty < x, \mu < \infty$ and $\sigma > 0$. Then using Equation (2.9), the CDF of the Gumbel-log-logistic{Cauchy} ($G$-$LL\{C\}$) distribution is defined as

$$F_X(x) = e^{-e^{-(\tan(u-\mu))/\sigma}},$$

and the corresponding PDF using Equation (2.10) is given by

$$f_X(x) = \frac{\alpha\pi}{\beta\sigma} \frac{(x/\beta)^{\alpha-1}}{(1+(x/\beta)^{\alpha})^2} e^{-(\tan(u-\mu))/\sigma} \sec^2(u)\, e^{-e^{-(\tan(u-\mu))/\sigma}},$$

where $u = \pi[(1+(x/\beta)^{-\alpha})^{-1} - 0.5]$, $x > 0$, $\alpha, \beta, \sigma > 0$, and $-\infty < \mu < \infty$.

Figure 4 illustrates different shapes of the PDF of $G$-$LL\{C\}$ for various values of $\alpha, \beta, \sigma$, and $\mu$. The graphs in Figure 4 indicate that the $G$-$LL\{C\}$ distribution can be unimodal (left skewed, symmetric, right skewed, monotonically decreasing (reversed J-shape)), or bimodal. Figure 4 also shows that the $G$-$LL\{C\}$ distribution could have three different modal points, namely, one mode at zero, one positive mode, or two different positive modes.

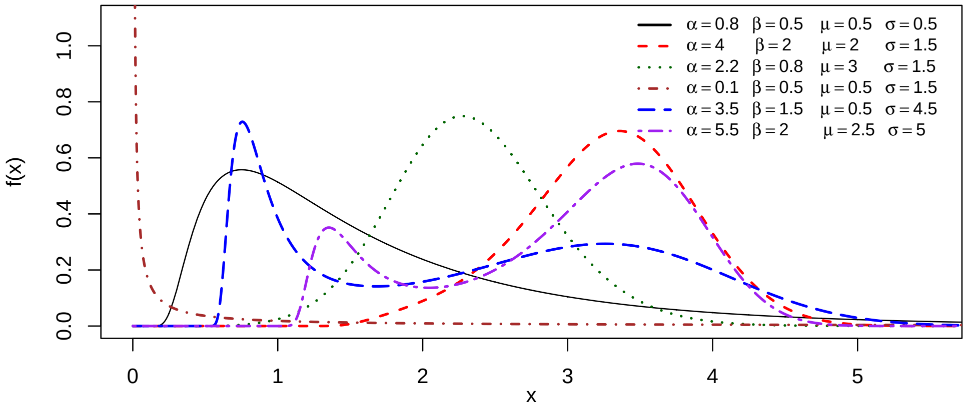


**Figure 4.** The PDFs of $G$-$LL\{C\}$ for various parameter values.

## 4.5. The normal-log-logistic{Cauchy} distribution

If the random variable $T$ follows the normal distribution with parameters $\mu$ (Shape) and $\sigma$ (Scale), then the CDF and PDF of the random variable $T$ are $F_T(x) = \Phi\left(\frac{x-\mu}{\sigma}\right)$ and $f_T(x) = \sigma^{-1}\phi\left(\frac{x-\mu}{\sigma}\right)$, where $\phi(x)$ is $N(\mu, \sigma)$, $\Phi(x)$ is the CDF of $\phi(x)$, $-\infty < x, \mu < \infty$ and $\sigma > 0$. Using Equation (2.9), the CDF of the normal-log-logistic{Cauchy}($N$-$LL\{C\}$) distribution is defined as

$$F_X(x) = \Phi(\tan(u - \mu)/\sigma)$$

and the corresponding PDF using Equation (2.10) is given by

$$f_X(x) = \frac{\alpha\pi}{\beta\sigma}\frac{(x/\beta)^{\alpha-1}}{(1 + (x/\beta)^{\alpha})^2}\sec^2(u)\phi(\tan(u - \mu)/\sigma),$$

where $u = \pi[(1 + (x/\beta)^{-\alpha})^{-1} - 0.5]$, $x > 0$ $x > 0$, $\alpha, \beta, \sigma > 0$, and $-\infty < \mu < \infty$.

Figure 5 provides graphs of the PDF of $N$-$LL\{C\}$ for various values of $\alpha, \beta, \sigma$, and $\mu$. Similar to the $L$-$LL\{C\}$ and $G$-$LL\{C\}$ distributions, the $N$-$LL\{C\}$ distribution exhibits unimodal (skewed to right, skewed to the left, symmetric, or reversed J-shape) or bimodal shapes.

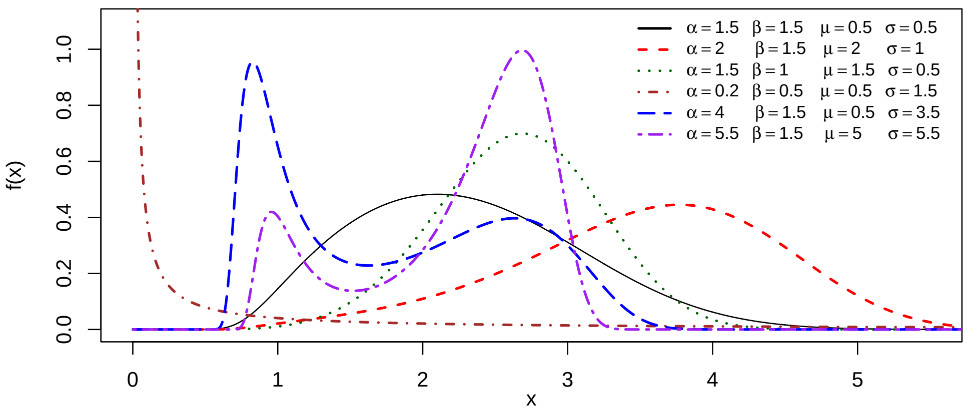


**Figure 5.** The PDFs of $N$-$LL\{C\}$ for various parameter values.

## 5. Estimation and simulation

In this section, we use the method of maximum likelihood to address the parameter estimation for the $N$-$LL\{C\}$ distribution and conduct a simulation to examine the performance of this method.

## 5.1. Estimation for the parameters of the *N-LL*$\{C\}$ distribution

Let $X_1, X_2, ..., X_n$ be a random sample of size $n$ drawn from the *N-LL*$\{C\}$ as defined in Subsection 4.5. Let $\Omega = (\alpha, \beta, \mu, \sigma)^T$ be a vector of parameters of dimension 4. By setting $z_i = 1 + (x_i/\beta)^\alpha$, the corresponding log-likelihood function for $\Omega$ is given by

$$\ell(\Omega) = n\log(\pi/2)^{1/2} + n\log(\alpha/\beta\sigma) + (\alpha-1)\sum_{i=1}^{n}\log(x_i/\beta)$$
$$-2\sum_{i=1}^{n}\log z_i + \sum_{i=1}^{n}\log\left(\csc\pi z_i^{-1}\right) - \frac{1}{2\sigma^2}\sum_{i=1}^{n}\left(\mu - \cot\pi\left(z_i^{-1}\right)\right)^2.$$

The derivatives of $\ell(\Omega)$ with respect to the parameters $\mu$ and $\sigma$ are given by, respectively, as

$$\partial\ell/\partial\mu = -\frac{2}{\sigma^2}\sum_{i=1}^{n}\left(\mu - \cot\pi\left(z_i^{-1}\right)\right) \tag{5.1}$$

and

$$\partial\ell/\partial\sigma = -\frac{n}{\sigma} + \frac{2}{\sigma^3}\sum_{i=1}^{n}\left(\mu - \cot\pi\left(z_i^{-1}\right)\right)^2. \tag{5.2}$$

By setting Equations (5.1) and (5.2) to zero, the maximum likelihood estimates (MLEs) $\hat{\mu}$ and $\hat{\sigma}$ of $\mu$ and $\sigma$ are given by

$$\hat{\mu} = \frac{1}{n}\sum_{i=1}^{n}\cot\pi\left(z_i^{-1}\right) \tag{5.3}$$

and

$$\hat{\sigma} = \sqrt{\frac{2}{n}\sum_{i=1}^{n}\left(\hat{\mu} - \cot\pi\left(z_i^{-1}\right)\right)^2} = \sqrt{\frac{2}{n}\sum_{i=1}^{n}\left(\left\{\frac{1}{n}\sum_{i=1}^{n}\cot\pi\left(z_i^{-1}\right)\right\} - \cot\pi\left(z_i^{-1}\right)\right)^2}, \tag{5.4}$$

respectively. Hence, to find the MLEs $\hat{\alpha}, \hat{\beta}, \hat{\mu}$, and $\hat{\sigma}$ of the parameters $\alpha, \beta, \mu$ and $\sigma$, we first substitute Equations (5.3) and (5.4) into the log-likelihood function $\ell(\Omega)$ and maximize it with respect to the parameters $\alpha$ and $\beta$, which gives the MLEs $\hat{\alpha}$ and $\hat{\beta}$. Then, substitute $\hat{\alpha}$ and $\hat{\beta}$ into Equation (5.3) to find the MLE $\hat{\mu}$ and then substitute $\hat{\alpha}$, $\hat{\beta}$ and $\hat{\mu}$ into Equation (5.4) to find the MLE $\hat{\sigma}$. The initial values for the parameters $\alpha$ and $\beta$ is obtained by assuming the random sample $x_i$, $i = 1, 2 \ldots, n$, is from log-logistic distribution with parameters $\alpha$ and $\beta$. The SAS software was used to run all the needed analysis.

## 5.2. Simulation for the parameters of the *N-LL*$\{C\}$ distribution

A simulation study is conducted to assess the performance of the MLEs for *N-LL*$\{C\}$ distribution in terms of the bias and standard deviation of the estimates for different parameter combinations and sample sizes. Based on Corollary 3.3 (*iii*), a random sample of size $n$ from a *N-LL*$\{C\}$ distribution can be simulated. Four sample sizes are considered ($n = 50, 100, 200, 500$). We use the same parameter combinations in Figure 5 to conduct this simulation. These combinations cover different shapes of the *N-LL*$\{C\}$ distribution, including, right skewed, symmetric, left skewed, and bimodal. For each sample size and each parameter combination, the process is repeated 1000 times to evaluate the MLE of $\Omega$. The bias and standard deviation of the MLE of $\Omega$ is reported in Table 2.

The results in Table 2 show that the ML method is appropriate for estimating the *N-LL*$\{C\}$ parameters. As expected, the biases and standard deviations of the MLEs seem to be reasonable and decrease as the sample size increases. It is clear that the MLEs are quite stable and close to the actual values of the parameters for large sample sizes.

**Table 2.** Bias and standard deviations for the $N$-$LL\{C\}$ parameters.

| Actual Values | | | | | Bias | | | | Standard deviation | | | |
|---|---|---|---|---|---|---|---|---|---|---|---|---|
| $\alpha$ | $\beta$ | $\mu$ | $\sigma$ | $n$ | $\hat{\alpha}$ | $\hat{\beta}$ | $\hat{\mu}$ | $\hat{\sigma}$ | $\hat{\alpha}$ | $\hat{\beta}$ | $\hat{\mu}$ | $\hat{\sigma}$ |
| $1.5^R$ | 1.5 | 0.5 | 0.5 | 50 | 0.5995 | 0.1638 | 0.0263 | 0.2790 | 0.7265 | 0.3522 | 0.3694 | 0.3414 |
| | | | | 100 | 0.3350 | 0.1134 | 0.0107 | 0.1473 | 0.5148 | 0.3041 | 0.2494 | 0.2191 |
| | | | | 200 | 0.1456 | 0.0348 | 0.0065 | 0.0665 | 0.3938 | 0.2673 | 0.1873 | 0.1583 |
| | | | | 500 | 0.0489 | 0.0033 | 0.0055 | 0.0232 | 0.2641 | 0.1845 | 0.1124 | 0.1006 |
| $2^L$ | 1.5 | 2 | 1 | 50 | 0.6830 | 0.5065 | 0.2132 | 0.2222 | 0.7208 | 0.5334 | 0.8736 | 0.4999 |
| | | | | 100 | 0.3575 | 0.3024 | 0.1556 | 0.1049 | 0.4813 | 0.4043 | 0.6640 | 0.3301 |
| | | | | 200 | 0.1798 | 0.1509 | 0.0531 | 0.0608 | 0.3459 | 0.3256 | 0.5204 | 0.2364 |
| | | | | 500 | 0.0652 | 0.0576 | 0.0253 | 0.0207 | 0.2107 | 0.2027 | 0.3224 | 0.1456 |
| $1^S$ | 1 | 1.5 | 0.5 | 50 | 1.1402 | 0.7826 | 0.4610 | 0.2242 | 0.7229 | 0.4191 | 0.6704 | 0.2838 |
| | | | | 100 | 0.9081 | 0.7051 | 0.5015 | 0.1388 | 0.6441 | 0.4017 | 0.5302 | 0.2042 |
| | | | | 200 | 0.6246 | 0.5539 | 0.4268 | 0.0752 | 0.4857 | 0.3404 | 0.4239 | 0.1496 |
| | | | | 500 | 0.3951 | 0.4064 | 0.3482 | 0.0299 | 0.2988 | 0.2606 | 0.3147 | 0.0911 |
| $4^B$ | 1.5 | 0.5 | 3.5 | 50 | 0.1745 | 0.0025 | 0.0590 | 0.5943 | 0.5800 | 0.0576 | 0.7525 | 1.7047 |
| | | | | 100 | 0.1140 | 0.0048 | 0.0255 | 0.3649 | 0.4076 | 0.0379 | 0.5018 | 1.1011 |
| | | | | 200 | 0.0540 | 0.0007 | 0.0199 | 0.1799 | 0.2908 | 0.0270 | 0.3583 | 0.7484 |
| | | | | 500 | 0.0222 | 0.0001 | 0.0062 | 0.0685 | 0.1741 | 0.0160 | 0.2035 | 0.4263 |
| $5.5^B$ | 1.5 | 5 | 5.5 | 50 | 0.0700 | 0.0149 | 0.0970 | 0.1431 | 0.6613 | 0.0645 | 1.3281 | 1.9502 |
| | | | | 100 | 0.0386 | 0.0073 | 0.0359 | 0.1673 | 0.4990 | 0.0423 | 1.1628 | 1.5757 |
| | | | | 200 | 0.0326 | 0.0032 | 0.0711 | 0.1362 | 0.3519 | 0.0289 | 0.9303 | 1.1230 |
| | | | | 500 | 0.0288 | 0.0020 | 0.0604 | 0.1080 | 0.2372 | 0.0173 | 0.6336 | 0.7655 |

R: Skewed to the right, S: symmetric, L: skewed to the left, B: bimodal distribution.

## 6. Applications

In this section, we provide six applications to illustrate the flexibility of the members of $T$-$LL\{Y\}$ family of distributions in fitting real-world data. In these applications, examples of unimodal and bimodal data sets arising from diverse disciplines are used to compare the fits of members of $T$-$LL\{Y\}$ distributions with other flexible distributions, namely, the beta normal ($BN$) [13], the Weibull-Gamma {log-logistic} ($W$-G$\{LL\}$ ) [4], and the Gumbel Weibull ($GW$) [1] distributions, based on the log-likelihood ($\log l$) value, the Kolmogorov-Smirnov (K-S) test statistic and its p-value, the Akaike information criterion (AIC), and the Bayesian Information Criterion (BIC). The competitor distributions were selected based on their ability to fit many unimodal and bimodal shapes (see [1, 4, 13]). More importantly, these distributions showed the best fit among other flexible distributions in some of the data sets used in this application section.

In addition, other test statistics such as Cramér-von Mises ($W^*$) and Anderson-Darling ($A^*$) are also provided (see [9] for more details). The method of maximum likelihood is applied to estimate the parameters of the fitted distribution using NLMIXED procedure in SAS.

### 6.1. Unimodal data sets

In this subsection, we present applications of the members of $T$-$LL\{Y\}$ family of distributions to three unimodal data sets with different levels of skewness. The distributions of these data sets are approximately symmetric, skewed to the right, and skewed to the left. In the first two applications, the four parameters $T$-$LL\{Y\}$ members: $W$-$LL\{E\}$, $L$-$LL\{C\}$, $G$-$LL\{C\}$, and $N$-$LL\{C\}$, are used to fit approximately symmetric and right-skewed data sets. In the third application, we apply the distributions: $EE$-$LL\{E\}$, $L$-$LL\{C\}$, $G$-$LL\{C\}$, and $N$-$LL\{C\}$ to model left skewed data set. To show the the usefulness of the members of $T$-$LL\{Y\}$ distributions in fitting real-life data, the goodness-of-fit results are compared with the $BN$ [13], the $W$-G$\{LL\}$ [4], and the $GW$ [1] distributions.

**6.1.1. Data 1: Oxford and Worthing annual maximum temperatures.** For our first example we consider a data set ($n = 80$) representing the annual maximum temperatures, from Oxford and Worthing in the U.K., for the years 1901 to 1980. The data is used by [8] and modeled using generalized extreme value marginal distributions. Recently, Alzaatreh et al. [4] used the data in an application of the $W$-$G\{LL\}$ distribution. The data is approximately symmetric (skewness = 0.0162 and kurtosis = 2.7309).

The MLEs and goodness-of-fit statistics are given in Tables 3 and 4, and the estimated PDFs, along with the histogram of the annual maximum temperatures are shown in Figure 6. The results in Table 4 indicate that all models fit the data almost equally well with some minor differences in the values of different statistics. However, based on the lowest AIC, BIC, and $-2\log l$ values, the $W$-$LL\{E\}$ and $G$-$LL\{C\}$ distributions provide the best fit to the data. It can also be seen in Table 4 that the $L$-$LL\{C\}$, $BN$, and $W$-$G\{LL\}$ distributions are competitive models and give the best fit to the data based on the smallest $K$-$S$, $W^*$ and $A^*$ statistics, respectively. This application suggests the applicability of modelling approximately symmetric unimodal data using some representative of the $T$-$LL\{Y\}$ family of distributions (see Figure 6).

**Table 3.** MLEs results for the annual maximum temperatures data (data 1).

| | Estimates (Standard error) | | | |
|---|---|---|---|---|
| Distribution | $\hat{\alpha}$ | $\hat{\beta}$ | $\hat{\mu}$ | $\hat{\sigma}$ |
| $W$-$LL\{E\}$ | 87.7615 | 70.8808 | 4.1748 | 17.7944 |
| | (19.4421) | (10.7813) | (3.4812) | (10.4005) |
| $L$-$LL\{C\}$ | 12.6726 | 84.0727 | 0.1530 | 0.3186 |
| | (4.5607) | (1.8163) | (0.2312) | (0.1428) |
| $G$-$LL\{C\}$ | 11.9117 | 76.7701 | 0.9512 | 0.7040 |
| | (4.3988) | (5.8019) | (0.6753) | (0.2134) |
| $N$-$LL\{C\}$ | 6.5403 | 81.9669 | 0.2091 | 0.2712 |
| | (7.2280) | (8.1051) | (0.3816) | (0.3123) |
| $BN$ | 58.3309 | 100.54 | 99.5393 | 41.6645 |
| | (449.28) | (304.80) | (491.90) | (703.66) |
| $W$-$G\{LL\}$ | 423.0032 | 0.2232 | 0.4753 | 0.0481 |
| | (169.64) | (0.0904) | (0.1934) | (0.1168) |
| $GW$ | 7.7912 | 14.4027 | 47.9726 | 29.1933 |
| | (2.0662) | (10.4547) | (76.588) | (1125.5) |

**Table 4.** Goodness-of-fit tests for the annual maximum temperatures data (data 1).

| | Statistics | | | | | |
|---|---|---|---|---|---|---|
| Distribution | $-2\log l$ | AIC | BIC | K-S (p-value) | $A^*$ | $W^*$ |
| $W$-$LL\{E\}$ | **457.7** | **465.7** | **475.3** | 0.0669 (0.8595) | 0.3195 | 0.0524 |
| $L$-$LL\{C\}$ | 457.8 | 465.8 | 475.3 | **0.0637** (**0.9019**) | 0.3087 | 0.0505 |
| $G$-$LL\{C\}$ | **457.7** | **465.7** | **475.2** | 0.0666 (0.8697) | 0.3185 | 0.0520 |
| $N$-$LL\{C\}$ | 457.9 | 465.9 | 475.4 | 0.0675 (0.8593) | 0.3243 | 0.0531 |
| $BN$ | 458.1 | 466.1 | 475.7 | 0.0638 (0.9007) | **0.3070** | 0.0504 |
| $W$-$G\{LL\}$ | 458.0 | 466.0 | 475.5 | 0.0640 (0.8987) | 0.3086 | **0.0502** |
| $GW$ | 458.5 | 466.5 | 476.0 | 0.0647 (0.8909) | 0.3132 | 0.0518 |

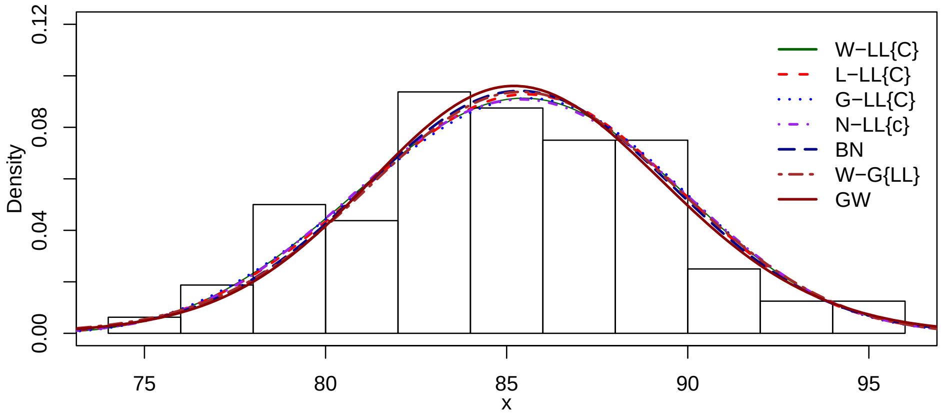


**Figure 6.** Fitted PDFs for the annual maximum temperatures data (data 1).

**6.1.2. Data 2: Australian Institute of Sport - sum of skin folds.** For this example, the data set ($n = 202$), which is obtained from [21], represents the sum of skin folds collected on a sample of 202 athletes at the Australian Institute of Sport. Alzaatreh et al. [4] applied the $W$-$G\{LL\}$ distribution to fit this data. The sum of skin folds for the 202 athletes is right skewed (skewness = 1.1660, kurtosis = 4.3220).

**Table 5.** MLEs results for for the sum of skin folds data (data 2).

| | Estimates (Standard error) | | | |
|---|---|---|---|---|
| Distribution | $\hat{\alpha}$ | $\hat{\beta}$ | $\hat{\mu}$ | $\hat{\sigma}$ |
| $W$-$LL\{E\}$ | 15.5005 | 25.8902 | 2.1145 | 15.4230 |
| | (0.2979) | (0.5331) | (0.1343) | (0.7501) |
| $L$-$LL\{C\}$ | 2.6186 | 70.8010 | −0.3696 | 0.7507 |
| | (0.2742) | (2.9594) | (0.1513) | (0.1375) |
| $G$-$LL\{C\}$ | 2.2142 | 56.6903 | −0.2091 | 0.8453 |
| | (0.2885) | (3.0665) | (0.1544) | (0.1725) |
| $N$-$LL\{C\}$ | 2.0588 | 75.6637 | −0.4028 | 0.9286 |
| | (0.2734) | (4.3471) | (0.1445) | (0.1904) |
| $BN$ | 163.77 | 0.2174 | −41.8560 | 29.4657 |
| | (36.3634) | (0.01651) | (1.8202) | (1.5935) |
| $W$-$G\{LL\}$ | 13.4018 | 10.4219 | 0.3184 | 0.0219 |
| | (2.7954) | (2.8058) | (2.8058) | (0.0131) |
| $GW$ | 3.2943 | 0.1738 | 111.05 | 1.4204 |
| | (0.9826) | (0.0863) | (14.4858) | (0.3634) |

**Table 6.** Goodness-of-fit tests for the sum of skin folds data (data 2).

| | Statistics | | | | | |
|---|---|---|---|---|---|---|
| Distribution | $-2\log l$ | AIC | BIC | K-S (p-value) | $A^*$ | $W^*$ |
| $W$-$LL\{E\}$ | 1898.2 | 1906.2 | 1919.5 | 0.0677 (0.9090) | 0.9164 | 0.1346 |
| $L$-$LL\{C\}$ | 1892.7 | 1900.7 | 1914.0 | **0.0356** (**0.9600**) | **0.3563** | **0.0372** |
| $G$-$LL\{C\}$ | **1889.6** | **1897.6** | **1910.8** | 0.0408 (0.8906) | 0.3582 | 0.0464 |
| $N$-$LL\{C\}$ | 1892.3 | 1900.3 | 1913.5 | 0.0396 (0.9091) | 0.3896 | 0.0442 |
| $BN$ | 1910.9 | 1918.9 | 1932.1 | 0.0872 (0.0928) | 1.9209 | 0.3553 |
| $W$-$G\{LL\}$ | 1924.4 | 1932.4 | 1945.6 | 0.0793 (0.1579) | 1.9923 | 0.3068 |
| $GW$ | 1897.9 | 1905.9 | 1919.2 | 0.0583 (0.4972) | 0.6875 | 0.1019 |

The MLEs and the goodness-of-fit statistics are provided in Tables 5 and 6. The histogram and the densities of the fitted distributions are depicted in Figure 7. By comparing the goodness-of-fit statistics among the seven distributions in Table 6, we observe that the $L$-$LL\{C\}$ distribution provides a better fit than the other fitted distributions based on the lowest $K$-$S$, $W^*$ and $A^*$ statistics, whereas the $G$-$LL\{C\}$ distribution provides the best fit based on the smallest $-2\log l$, AIC, and BIC values. This application shows the ability of some members of the $T$-$LL\{Y\}$ family of distributions in providing a good fit for a right skewed data set.

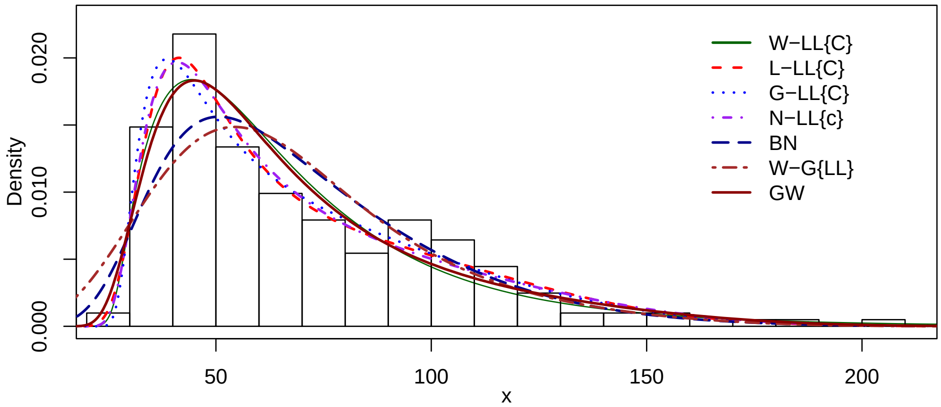


**Figure 7.** Fitted PDFs for the sum of skin folds data (data 2).

**6.1.3. Data 3: Turbocharger failure.** The data set is taken from [23] and it is about the time-to-failure for 40 suits of turbochargers in diesel engines. Alzaatreh et al. [4] also analyzed this data using the $W$-$G\{LL\}$ distribution. The distribution of this data is skewed to the left (skewness $= -0.6542$, kurtosis $= 2.5750$). Tables 7 and 8 provide the estimates of the model parameters and their standard errors, and goodness-of-fit statistics for all seven models. Here, we see that the $EE$-$LL\{E\}$ distribution outperforms the other distributions (based on the lowest values of all measures in Table 8) and provide the best fit to the time to failure of turbocharger's data. This application suggests that the $EE$-$LL\{E\}$ distribution is capable to fit left skewed data. The plots in Figure 8 support the results of Table 8 in showing that the $EE$-$LL\{E\}$ distribution provides the best fit to this left skewed histogram.

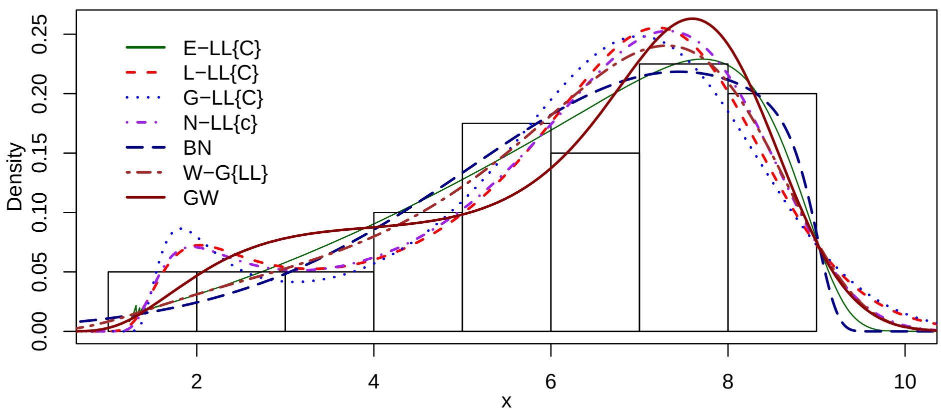


**Figure 8.** Fitted PDFs for failure of turbocharger data (data 3).

**Table 7.** MLEs results for failure of turbocharger data (data 3).

| | Estimates (Standard error) | | | |
|---|---|---|---|---|
| Distribution | $\hat{\alpha}$ | $\hat{\beta}$ | $\hat{\mu}$ | $\hat{\sigma}$ |
| *EE-LL*$\{E\}$ | 17.4700 | 10.5459 | 0.1459 | 0.02864 |
| | (0.7172) | (0.7545) | (0.02444) | (0.03090) |
| *L-LL*$\{C\}$ | 3.2623 | 3.4349 | 2.9742 | 1.4997 |
| | (0.6794) | (0.3621) | (1.3205) | (0.7940) |
| *G-LL*$\{C\}$ | 3.8369 | 3.0267 | 4.5733 | 5.3864 |
| | (0.6500) | (0.2699) | (2.1193) | (2.6199) |
| *N-LL*$\{C\}$ | 3.1643 | 3.2113 | 3.4372 | 2.7513 |
| | (0.6435) | (0.3644) | (1.4730) | (1.3572) |
| *BN* | 0.03019 | 171.28 | 10.4407 | 0.5442 |
| | (0.0433) | (1.2995) | (1.0860) | (0.4682) |
| *W-G*$\{LL\}$ | 7.5745 | 0.5396 | 0.6094 | 28.3338 |
| | (5.5233) | (0.3396) | (0.2749) | (43.2957) |
| *GW* | 6.3478 | 1.2516 | 5.5313 | 5.8421 |
| | (2.6649) | (0.5420) | (0.9687) | (1.7686) |

**Table 8.** Goodness-of-fit tests for failure of turbocharger data (data 3).

| | Statistics | | | | | |
|---|---|---|---|---|---|---|
| Distribution | $-2\log l$ | AIC | BIC | K-S (p-value) | $A^*$ | $W^*$ |
| *EE-LL*$\{E\}$ | **156.4** | **164.4** | **171.1** | **0.0703 (0.9665)** | **0.1494** | **0.0204** |
| *L-LL*$\{C\}$ | 159.0 | 167.0 | 173.7 | 0.0821 (0.9502) | 0.2623 | 0.0403 |
| *G-LL*$\{C\}$ | 158.9 | 166.9 | 173.7 | 0.0927 (0.8819) | 0.2966 | 0.0447 |
| *N-LL*$\{C\}$ | 157.1 | 165.1 | 171.9 | 0.0784 (0.9665) | 0.2303 | 0.0370 |
| *BN* | 156.6 | 164.6 | 171.4 | 0.0743 (0.9800) | 0.1606 | 0.0226 |
| *W-G*$\{LL\}$ | 157.9 | 165.9 | 172.7 | 0.0820 (0.9507) | 0.2342 | 0.0332 |
| *GW* | 158.4 | 166.4 | 173.1 | 0.0821 (0.9501) | 0.2009 | 0.0305 |

## 6.2. Bimodal data sets

Recall that the *L-LL*$\{C\}$, *G-LL*$\{C\}$, and *N-LL*$\{C\}$ distributions exhibit different shapes including bimodal. In the following applications, three examples of bimodal data sets are provided comparing the fits of these distributions with the models used in previous subsections, namely, the *BN*, the *W*-G$\{LL\}$, and the *GW* distributions.

**6.2.1. Data 4: Egg sizes in asteroids and echinoids.** In this application, the data set with $n = 88$ is on the asteroid and echinoid egg size taken from [11]. This data contains 88 asteroids species divided into three types; 35 planktotrophic larvae, 36 lecithotrophic larvae, and 17 brooding larvae. The histogram of the logarithm of the egg diameters of the asteroids data shows a bimodal shape (see Figure 9). Fomaye et al. [13] and Alzaatreh et al. [4] used the *BN* and *W-G*$\{LL\}$ distributions, respectively, to analyze this data.

The MLEs and goodness-of-fit statistics are given in Tables 9 and 10, and the estimated PDFs are shown in Figure 9. Recall that all of these distributions have the ability to fit a bimodal data. The goodness of fit statistics show that the *G-LL*$\{C\}$ distribution provides the best fit to the data, followed successively by the *L-LL*$\{C\}$ and *N-LL*$\{C\}$ distributions. This application is a good illustration of the power of the members of *T-LL*$\{Y\}$ family of distributions in modeling bimodal data sets. The plots in Figure 9 reveal that the *G-LL*$\{C\}$, *L-LL*$\{C\}$, and *N-LL*$\{C\}$ distributions provide adequate fits to the data, and this is in agreement with the results in Table 10.

**Table 9.** MLEs results for asteroid and echinoid egg size data (data 4).

| | Estimates (Standard error) | | | |
|---|---|---|---|---|
| Distribution | $\hat{\alpha}$ | $\hat{\beta}$ | $\hat{\mu}$ | $\hat{\sigma}$ |
| *L-LL*{*C*} | 11.1691 | 5.9795 | −0.0413 | 1.6657 |
| | (1.1923) | (0.0671) | (0.3743) | (0.4367) |
| *G-LL*{*C*} | 11.0246 | 5.7972 | −0.5612 | 2.4274 |
| | (1.1724) | (0.0647) | (0.4073) | (0.6396) |
| *N-LL*{*C*} | 9.4711 | 6.0377 | −0.1338 | 2.0786 |
| | (1.1336) | (0.0761) | (0.3139) | (0.5547) |
| *BN* | 0.0129 | 0.007 | 5.7466 | 0.0675 |
| *W-G*{*LL*} | 410.7779 | 0.0151 | 0.1390 | 3.6233 |
| | (16.1145) | (0.0196) | (0.0865) | (0.4476) |
| *GW* | 11.4586 | 0.3900 | 6.7407 | 2.1196 |
| | (3.0482) | (0.1776) | (0.3007) | (0.4817) |

**Table 10.** Goodness-of-fit tests for asteroid and echinoid egg size data (data 4).

| | Statistics | | | | | |
|---|---|---|---|---|---|---|
| Distribution | $-2\log l$ | AIC | BIC | K-S (p-value) | $A^*$ | $W^*$ |
| *L-LL*{*C*} | 216.7 | 224.7 | 234.6 | 0.0884 (0.4980) | 0.8401 | 0.1286 |
| *G-LL*{*C*} | **210.7** | **218.7** | **228.6** | **0.0868 (0.5211)** | **0.6888** | **0.1050** |
| *N-LL*{*C*} | 218.4 | 226.4 | 236.3 | 0.0942 (0.4151) | 0.9724 | 0.1623 |
| *BN* | 218.5 | 226.96 | 236.4 | 0.1233 (0.1377) | 2.6282 | 0.4532 |
| *W-G*{*LL*} | 222.4 | 230.4 | 240.3 | 0.1088 (0.2486) | 2.1584 | 0.2231 |
| *GW* | 233.7 | 241.7 | 251.6 | 0.1427 (0.0555) | 1.8502 | 0.3245 |

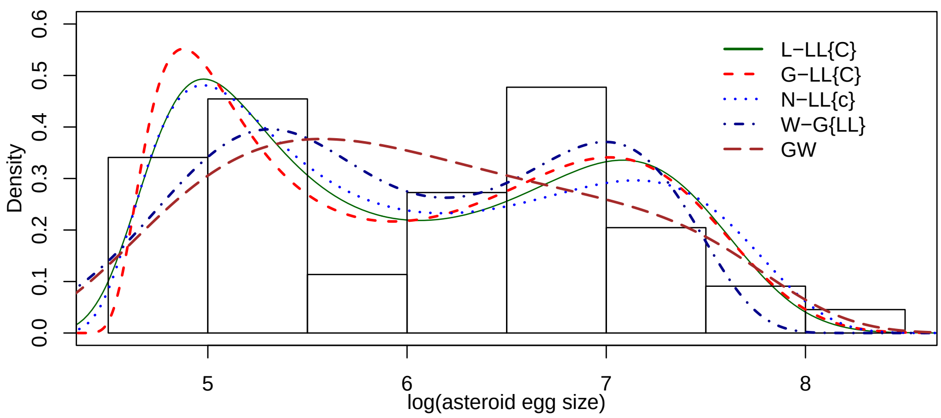


**Figure 9.** Fitted PDFs for asteroid and echinoid egg size data (data 4).

**6.2.2. Data 5: Old faithful geyser - waiting time between eruptions.** The old faithful geyser data consists of 272 observations on 2 variables. The variables are: the waiting time between eruptions and the duration of the eruption for the old faithful geyser in Yellowstone National Park, Wyoming, USA (see [6,15] for more details). This application considers the waiting time between eruptions for the old faithful geyser. We will also be using the duration of the eruption variable in the next application.

The MLEs and goodness of fit statistics are given in Tables 11 and 12. Based on all measures in Table 12, the results show that the *L-LL*{*C*} distribution is superior to the other five distributions. Note also that the *N-LL*{*C*} has the second-lowest values of

$-2\log l$, AIC, and BIC, and the *G-LL*$\{C\}$ distribution has the second-lowest values of *K-S*, $W^*$ and $A^*$ statistics. As seen in the previous application, the three bimodal members of the *T-LL*$\{Y\}$ family of distributions can be used effectively to fit bimodal data sets with major mode and minor mode. Figure 10 displays the histogram of the waiting times between eruptions as well as the PDFs for the fitted distributions.

**Table 11.** MLEs results for the waiting time between eruptions data (data 5).

| | Estimates (Standard error) | | | |
|---|---|---|---|---|
| Distribution | $\hat{\alpha}$ | $\hat{\beta}$ | $\hat{\mu}$ | $\hat{\sigma}$ |
| *L-LL*$\{C\}$ | 9.5346 | 63.2263 | 1.6928 | 2.1531 |
| | (0.5576) | (0.5019) | (0.3344) | (0.3461) |
| *G-LL*$\{C\}$ | 9.2598 | 59.9996 | 1.1714 | 3.7915 |
| | (0.5200) | (0.4715) | (0.5971) | (0.3360) |
| *N-LL*$\{C\}$ | 8.1915 | 62.5395 | 1.3868 | 2.7165 |
| | (0.5050) | (0.5730) | (0.2702) | (0.4156) |
| *BN* | 0.1168 | 0.09122 | 67.7061 | 3.4928 |
| | (0.0173) | (0.0068) | (1.1115) | (0.1474) |
| *W-G*$\{LL\}$ | 134.61 | 0.4924 | 0.2239 | 46.5283 |
| | (0.1538) | (0.0081) | (0.0128) | (31.5341) |
| *GW* | 12.2779 | 0.8522 | 72.3542 | 4.1707 |
| | (1.1927) | (0.1150) | (1.3698) | (0.4246) |

**Table 12.** Goodness-of-fit tests for the waiting time between eruptions data (data 5).

| | Statistics | | | | | |
|---|---|---|---|---|---|---|
| Distribution | $-2\log l$ | AIC | BIC | K-S (p-value) | $A^*$ | $W^*$ |
| *L-LL*$\{C\}$ | **2074.5** | **2082.5** | **2096.9** | **0.0475 (0.5717)** | **0.5631** | **0.0918** |
| *G-LL*$\{C\}$ | 2083.3 | 2091.3 | 2105.8 | 0.0514 (0.4691) | 0.7750 | 0.1362 |
| *N-LL*$\{C\}$ | 2081.9 | 2089.9 | 2104.3 | 0.0587 (0.3062) | 0.9003 | 0.1592 |
| *BN* | 2137.4 | 2145.4 | 2159.9 | 0.1403 (0.0001) | 5.4169 | 1.0923 |
| *W-G*$\{LL\}$ | 2103.2 | 2111.2 | 2125.7 | 0.0696 (0.1433) | 1.6118 | 0.2740 |
| *GW* | 2109.7 | 2117.7 | 2132.1 | 0.0739 (0.1024) | 2.0127 | 0.3424 |

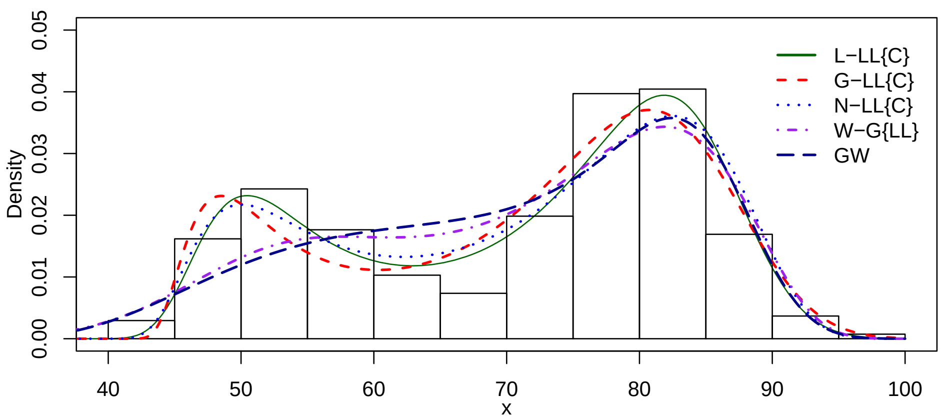


**Figure 10.** Fitted PDFs for the waiting time between eruptions data (data 5).

**6.2.3. Data 6: Old faithful geyser - duration of the eruption.** The duration of the eruption (in minutes) for the old faithful geyser is considered in this application. Among the fitted distributions, it seems that the $L$-$LL\{C\}$ distribution provides the best fit to the data with smallest $-2\log l$, AIC, BIC, AIC, $W^*$, and $A^*$ values. However, $N$-$LL\{C\}$ provides the best fit based on the $K$-$S$ statistic and its corresponding p-value. From applications 4 and 5, we observe that the $G$-$LL\{C\}$ distribution gives adequate fit and seems to be very competitive to other bimodal distributions. Plots of the estimated PDFs are displayed in Figure 11. It is clear from these plots that the three bimodal representatives of the $T$-$LL\{Y\}$ family of distributions provide the best fit to the histogram of the duration of the eruption data.

**Table 13.** MLEs results for the duration of the eruption data (data 6).

| | Estimates (Standard error) | | | |
|---|---|---|---|---|
| Distribution | $\hat{\alpha}$ | $\hat{\beta}$ | $\hat{\mu}$ | $\hat{\sigma}$ |
| $L$-$LL\{C\}$ | 9.6482 | 2.8711 | 2.8711 | 13.2494 |
| | (0.4873) | (0.0184) | (2.1918) | (2.1918) |
| $G$-$LL\{C\}$ | 9.1180 | 2.7478 | 2.6697 | 18.5860 |
| | (0.4309) | (0.0165) | (1.5210) | (4.0169) |
| $N$-$LL\{C\}$ | 8.7864 | 2.8526 | 6.1087 | 15.9315 |
| | (0.4324) | (0.0187) | (1.6359) | (3.3943) |
| $BN$ | 0.06226 | 171.24 | 6.2182 | 0.4791 |
| | (0.0211) | (0.3620) | (0.2390) | (0.1012) |
| $W$-$G\{LL\}$ | 84.4827 | 0.03567 | 0.1411 | 675.41 |
| | (0.0318) | (0.0005) | (0.0076) | (394.64) |
| $GW$ | 12.927 | 0.7505 | 3.7903 | 8.0089 |
| | (1.1625) | (0.0831) | (0.0719) | (0.8103) |

**Table 14.** Goodness-of-fit tests for the duration of the eruption data (data 6).

| | Statistics | | | | | |
|---|---|---|---|---|---|---|
| Distribution | $-2\log l$ | AIC | BIC | K-S (p-value) | $A^*$ | $W^*$ |
| $L$-$LL\{C\}$ | **518.3** | **526.3** | **540.7** | 0.0308 (0.9581) | **0.2047** | **0.0258** |
| $G$-$LL\{C\}$ | 532.9 | 540.9 | 555.3 | 0.0405 (0.7642) | 0.3605 | 0.0378 |
| $N$-$LL\{C\}$ | 520.4 | 528.4 | 542.8 | **0.0267** (**0.9902**) | 0.2339 | 0.0314 |
| $BN$ | 760.9 | 768.9 | 783.3 | 0.1682 (0.0000) | 11.640 | 1.9421 |
| $W$-$G\{LL\}$ | 652.8 | 660.8 | 675.3 | 0.1203 (0.0008) | 6.9931 | 1.1829 |
| $GW$ | 652.7 | 660.7 | 675.1 | 0.1226 (0.0006) | 4.6004 | 0.6746 |

## 7. The $W$-$LL\{E\}$ parametric regression model with censored data

In this section, we develop a generalized parametric regression model for lifetime data with covariates, namely, the $W$-$LL\{E\}$ regression model. We also provide an example to illustrate the flexibility of the $W$-$LL\{E\}$ distribution in fitting right censored lifetime data set.

### 7.1. The $W$-$LL\{E\}$ parametric regression model

In the analysis of most lifetime data, the relationship between the covariates and the lifetime variable is of interest. One representation of this relationship is the linear relationship between the log lifetime variable and the covariate values, which can be described as follows:

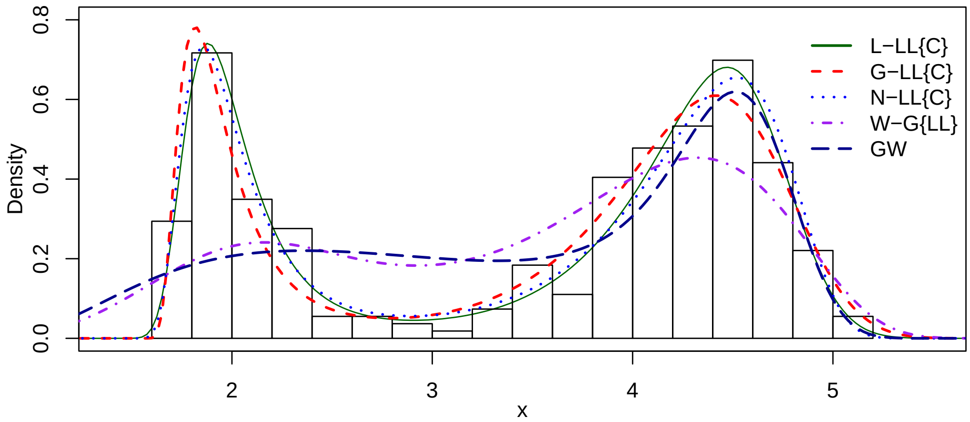


**Figure 11.** Fitted PDFs for the duration of the eruption data (data 6).

Let $X$ denote the lifetime variable and $\boldsymbol{Z}$ a vector of $p$ covariates such that $\boldsymbol{Z} = (1, z_{1,...,} z_p)^T$. The log-linear regression model which links the dependent variable $Y = \log(X)$ and the $p$ set of covariates is given by

$$Y = \log(X) = \boldsymbol{\gamma}^T \boldsymbol{Z} + \tau W, \tag{7.1}$$

where $\boldsymbol{\gamma}^T = (\gamma_0, \gamma_1, ..., \gamma_p)$ is a vector of regression coefficients, $\tau$ is an unknown scale parameter, and $W$ is the error variable. Different distributions of $W$ imply different models of $X$. For example, logistic, extreme value, normal or generalized extreme value distributions lead to log-logistic, Weibull, log-normal, or generalized gamma models for $X$. In this section, we derive a new generalized log-logistic model, called the $W$-$LL\{E\}$ regression model, for which $W$ has a standard log-$W$-$LL\{E\}$ distribution.

Suppose that a lifetime variable $X$ follows the $W$-$LL\{E\}$ distribution in Equation (4.1), then the survival function for the $W$-$LL\{E\}$ distribution is given by

$$S_X(x) = e^{-\left[\frac{1}{\sigma}\log\left(1+\left(\frac{x}{\beta}\right)^{\alpha}\right)\right]^{\mu}},$$

where $x > 0$ and $\alpha, \beta, \sigma, \mu > 0$.

Taking the log transform of $X$, and redefine the parameters as $\alpha = 1/\tau$ and $\beta = e^{\lambda}$, then, $Y = \log(X)$, can be written as a log linear model, $Y = \lambda + \tau W$, where the random variable $W = (Y - \lambda)/\tau$ has a standard log-$W$-$LL\{E\}$ distribution with PDF

$$\pi_W(w) = \frac{\mu}{\sigma}\frac{e^w}{1+e^w}\left[\frac{1}{\sigma}\log(1+e^w)\right]^{\mu-1} e^{-\left[\frac{1}{\sigma}\log(1+e^w)\right]^{\mu}}.$$

Thus, the underlying PDF and survival function, respectively, for $Y$ are

$$g_Y(y) = \frac{\mu}{\sigma\tau}\frac{e^{\left(\frac{y-\lambda}{\tau}\right)}}{1+e^{\left(\frac{y-\lambda}{\tau}\right)}}\left[\frac{1}{\sigma}\log\left(1+e^{\left(\frac{y-\lambda}{\tau}\right)}\right)\right]^{\mu-1} e^{-\left[\frac{1}{\sigma}\log\left(1+e^{\left(\frac{y-\lambda}{\tau}\right)}\right)\right]^{\mu}} \tag{7.2}$$

and

$$S_Y(y) = e^{-\left[(1/\sigma)\log\left(1+e^{\left(\frac{y-\lambda}{\tau}\right)}\right)\right]^{\mu}},$$

where $y \in \mathbb{R}$, $\lambda \in \mathbb{R}$ and $\tau, \sigma, \mu > 0$.

Plots of the log-$W$-$LL\{E\}$ density function in Equation (7.2) for some parameter values are given in Figure 12.

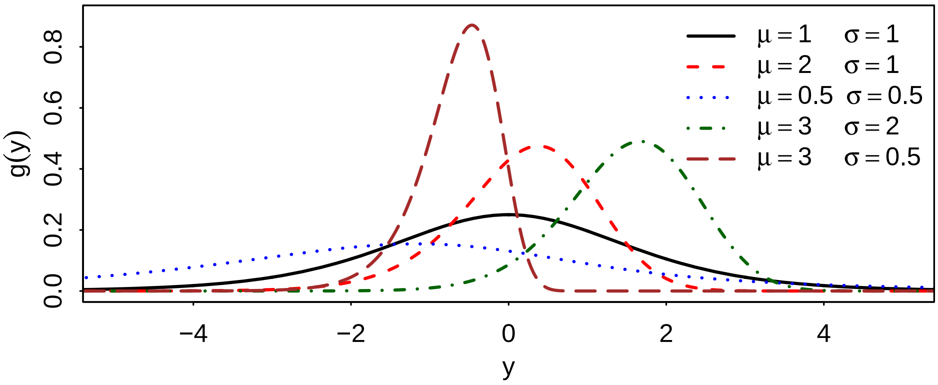


**Figure 12.** The PDFs of log-$W$-$LL\{E\}$ for various parameter values when $(\lambda, \tau) = (0, 1)$.

In order to incorporate covariates into the $W$-$LL\{E\}$ regression model, we use the log-linear model in Equation (7.1) for the lifetime $X$, where $W$ has a standard log-$W$-$LL\{E\}$ distribution such that $\lambda = \boldsymbol{\gamma}^T \boldsymbol{Z}$ is the location parameter of $Y$ and $\tau, \sigma, \mu > 0$ are unknown parameters. With the regression model in Equation (7.1), the survival function for $Y$ can be expressed as

$$S_Y(y|\boldsymbol{Z}) = e^{-\left[(1/\sigma)\log\left(1+e^{\left(\frac{y-\boldsymbol{\gamma}^T\boldsymbol{Z}}{\tau}\right)}\right)\right]^{\mu}}.$$

Now assume that we have $n$ independent individuals and let the random variables $X_i$ and $C_i$ denote the lifetime and censoring time of $i$th individual $(i = 1, ..., n)$. Let the response $Y_i$ represents a log-lifetime or a log-censoring time for $i$th individual such that $Y_i$= min $(\log(X_i), \log(C_i))$. Assume first that all the observations are uncensored, then the log likelihood for the model parameters $\boldsymbol{\theta} = (\mu, \sigma, \tau, \boldsymbol{\gamma}^T)^T$ is given by

$$l(\boldsymbol{\theta}) = \sum_{i=1}^{n} \log(g(y_i)) = n \log\left(\frac{\mu}{\sigma\tau}\right) + \sum_{i=1}^{n} w_i - \sum_{i=1}^{n} l(w_i) + (\mu - 1) \sum_{i=1}^{n} \log\left(\frac{1}{\sigma} l(w_i)\right) - \sum_{i=1}^{n} \left(\frac{1}{\sigma} l(w_i)\right)^{\mu},$$

where $w_i = (y_i - \gamma^T z_i)/\tau$ and $l(w_i) = \log(1 + e^{w_i})$. If some of the observations are right censored, then let $U_c$ and $U_u$ be the sets of censored and uncensored observations, respectively. Additionally, if we assume non-informative and independent censoring, then the log-likelihood function for the model parameters $\boldsymbol{\theta} = (\mu, \sigma, \tau, \boldsymbol{\gamma}^T)^T$ is given by

$$\begin{aligned} l(\boldsymbol{\theta}) &= \sum_{i\in U_u} \log(g(y_i)) + \sum_{i\in U_c} \log(S(y_i)) \\ &= m \log\left(\frac{\mu}{\sigma\tau}\right) + \sum_{i\in U_u} w_i - \sum_{i\in U_u} l(w_i) + (\mu - 1) \sum_{i\in U_u} l(w_i) - \sum_{i\in U_u} \left(\frac{1}{\sigma} l(w_i)\right)^{\mu} - \sum_{i\in U_c} \left(\frac{1}{\sigma} l(w_i)\right)^{\mu} \\ &= m \log\left(\frac{\mu}{\sigma\tau}\right) + \sum_{i\in U_u} w_i - \sum_{i\in U_u} l(w_i) + (\mu - 1) \sum_{i\in U_u} l(w_i) - \sum_{i=1}^{n} \left(\frac{1}{\sigma} l(w_i)\right)^{\mu}, \qquad (7.3) \end{aligned}$$

where $m$ is the number of uncensored observations. Once maximum likelihood estimate of the vector of parameters $\boldsymbol{\theta} = (\mu, \sigma, \tau, \boldsymbol{\gamma}^T)^T$ is computed, estimate of the survival function is available for the distribution of $Y$. Estimate of $\boldsymbol{\theta}$ can be found numerically, and routines to do so are available in most statistical packages. In the following application, NLMIXED procedure in SAS is used to obtain estimate of $\boldsymbol{\theta}$.

## 7.2. Application: Head-and-neck cancer study

In this real data application, we apply the $W$-$LL\{E\}$ regression model to fit right censored data from two arms of the Northern California Oncology Group (NCOG) study of head and neck cancer, which previously analyzed by [10]. This study compares treatment for head and neck cancer using radiotherapy alone (Arm A) with treatment for head and neck cancer using radiotherapy plus chemotherapy (Arm B). Of the 51 patients assigned to Arm A; 9 of them lost to follow-up (censored) and a total of 45 patients were enrolled in Arm B; 14 of them lost to follow-up. The survival time for each patient (measured in days) is the response variable.

Let $Y_i$ be the log survival time (in days) for the $i$th patient and $z_{i1}$ be the binary covariate: two-arm (Arm A = 0, Arm B = 1). We fit the *W-LL*$\{E\}$, log-logistic, generalized gamma, Weibull, and log-normal regression models to this data. The log linear model is given by

$$Y_i = \gamma_0 + \gamma_1 z_{i1} + \tau W_i;\ i = 1, 2, \ldots, 96,$$

where the random variable $W_i$ has the appropriate distribution for each of the five models.

It is clear that log-logistic distribution is a special case of *W-LL*$\{E\}$ distribution when $\mu = \sigma = 1$. Note also that the generalized gamma model includes the Weibull and the log-normal models as limiting cases. For the generalized gamma model, $Y = \log(X)$ follows the log linear model in Equation (7.1) with $W$ having the following PDF:

$$\pi(w) = \frac{|\theta|}{\Gamma(\theta^{-2})}\left(\theta^{-2}e^{\theta w}\right)^{\theta^{-2}}\left(e^{-e^{\theta w}/\theta^2}\right),$$

where $\Gamma(a)$ is the complete gamma function, and $-\infty < w < \infty$.

This regression model reduces to the Weibull model when $\theta = 1$, and, when $\theta = 0$, the model reduces to the log-normal model.

The estimates of the model parameters and their corresponding standard errors, the maximized likelihoods, and AIC and BIC criteria for all five models are provided in Table 15. The results indicate that the *W-LL*$\{E\}$ model has the lowest AIC and BIC values among the other fitted models, in that sense, is the best fitting model to this data. We see from the fitted *W-LL*$\{E\}$ regression model that there is no evidence of any difference in survival between Arm A and Arm B clinical trial.

**Table 15.** MLEs and fit statistics for the two-arm data (standard error) [p-value].

| Model | $\mu$ | $\sigma$ | $\tau$ | $\gamma_0$ | $\gamma_1$ | $-2\log l$ | AIC | BIC |
|---|---|---|---|---|---|---|---|---|
| *W-LL*$\{E\}$ | 0.5428 | 3.9953 | 0.2316 | 4.9939 | 0.1438 | **272.7** | **282.7** | **295.5** |
| | (0.1673) | (1.4172) | (0.0708) | (0.2354) | (0.1948) | | | |
| | | | | [< .0001] | [0.4622] | | | |
| *log-logistic* | 1 | 1 | 0.7585 | 5.4943 | 0.5549 | 288.1 | 294.1 | 301.8 |
| | | | (0.0736) | (0.1810) | (0.2779) | | | |
| | | | | [< .0001] | [0.0459] | | | |
| Model | | $\theta$ | $\tau$ | $\gamma_0$ | $\gamma_1$ | $-2\log l$ | AIC | BIC |
| *Generalized* | | −0.5723 | 1.2978 | 5.2294 | 0.5690 | 283.6 | 291.6 | 301.9 |
| *gamma* | | (0.2974) | (0.1108) | (0.2533) | (0.2681) | | | |
| | | | | [< .0001] | [0.0338] | | | |
| *Weibull* | | 1 | 1.1757 | 6.0387 | 0.7860 | 303.4 | 309.4 | 317.1 |
| | | | (0.1083) | (0.1821) | (0.2789) | | | |
| | | | | [< .0001] | [0.0048] | | | |
| *log-normal* | | 0 | 1.2933 | 5.5372 | 0.6177 | 286.9 | 292.9 | 300.6 |
| | | | (0.1122) | (0.1867) | (0.2744) | | | |
| | | | | [< .0001] | [0.0244] | | | |

A comparison of the *W-LL*$\{E\}$ regression model with its sub-model using likelihood ratio statistics in Table 16 indicates that the extra parameters $(\mu, \sigma)$ of the *W-LL*$\{E\}$ are jointly significant. Thus, the *W-LL*$\{E\}$ model is more flexible, due to two extra parameters, and outperforms the log-logistic model in fitting this data.

**Table 16.** Likelihood ratio test for the two-arm data.

| Model | Hypotheses | LR statistic | p-value |
|---|---|---|---|
| *W-LL*$\{E\}$ *vs log-logistic* | $H_0 : (\mu, \sigma) = (1, 1)$ *vs* $H_1 : H_0$ *is false* | 15.4 | 0.00045 |

The plots of the empirical survival function and the estimated survival functions of the *W-LL*$\{E\}$, log-logistic, and log-normal are depicted in Figure 13. These plots suggest that the *W-LL*$\{E\}$ model is appropriate to fit this data, so it can be considered a very competitive model to other lifetime models.

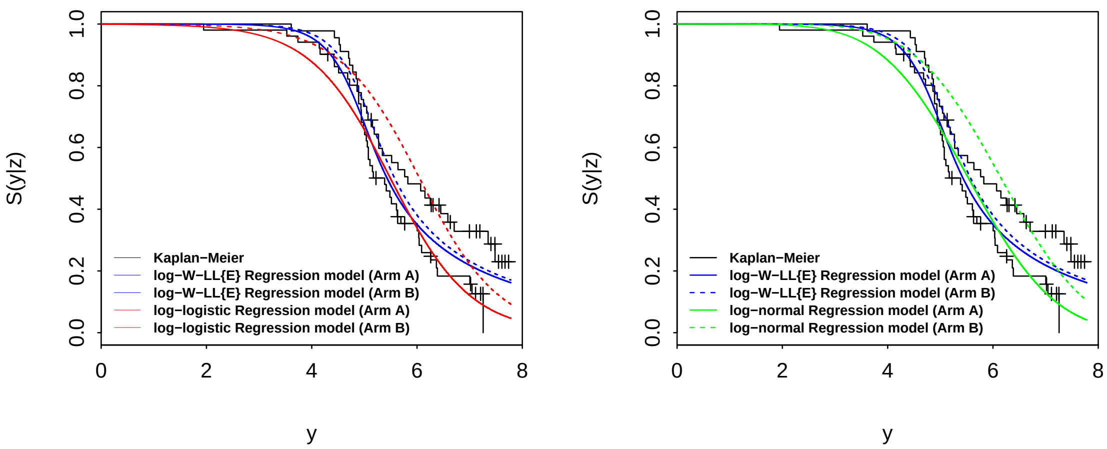


**Figure 13.** The empirical and estimated survival functions of the *W-LL*$\{E\}$, log-logistic, and log-normal for the Head-and-Neck Cancer data.

## 8. Summary and conclusions

In this paper, we discussed three members of the *T-LL*$\{Y\}$ family of distributions, namely the *T-LL*$\{E\}$, *T-LL*$\{L\}$, and *T-LL*$\{C\}$ classes of distributions. Several useful properties of these classes are introduced and studied in details. Five generalizations of the log-logistic distribution namely, the *W-LL*$\{E\}$, *EE-LL*$\{E\}$, *L-LL*$\{C\}$, *G-LL*$\{C\}$, and *N-LL*$\{C\}$ distributions were derived and studied. The maximum likelihood method is proposed to estimate the distributions parameters and a simulation study is carried out to measure the performance of the *N-LL*$\{C\}$ parameters. Based on the simulation results, it can be seen that the maximum likelihood method performs reasonably well and the MLEs get better with the increase in sample size. To illustrate the usefulness and flexibility of these distributions in applications, six real-world data sets arising from diverse branches of science with different sample sizes and different shapes are used. From the results of goodness-of-fit tables in Subsections 7.1 and 7.2, it is noticed that these generalized log-logistic distributions performed very well in fitting approximately symmetric, left skewed, right skewed, or bimodal data sets. A new generalized log-logistic lifetime model, the *W-LL*$\{E\}$ regression model, is derived and applied to fit a right censored data with covariates. The flexibility provided by this model could be very helpful in describing and explaining different types of lifetime data.

**Acknowledgment.** The authors would like to thank the editor and anonymous referees for their valuable comments and suggestions that improved the quality of the paper.

## References

[1] R. Al-Aqtash, C. Lee and F. Famoye, *Gumbel-weibull distribution: Properties and applications*, J. Mod. Appl. Stat. Methods **13** (2), 201-255, 2014.

[2] A. Aljarrah, C. Lee and F. Famoye, *On generating T-X family of distributions using the quantile function*, J. Stat. Distrib. Appl. **1** (2), 1-17, 2014.

[3] A. Alzaatreh, C. Lee and F. Famoye, *A new method for generating families of continuous distributions*, Metron **71** (1), 63-79, 2013.

[4] A. Alzaatreh, C. Lee and F. Famoye, *Family of generalized gamma distributions: Properties and applications*, Hacet. J. Math. Stat. **45** (3), 869-886, 2015.

[5] B.C. Arnold, H.W. Gómez, and H.S. Salinas, *A doubly skewed normal distribution*, Statistics **49** (4), 842-858, 2015.

[6] A. Azzalini and A. W. Bowman, *A look at some data on the old faithful geyser*, J. R. Stat. Soc. Ser. C. Appl. Stat. **39**, 357-365, 1990.

[7] E.F. Bell, C. Wolf, K. Meisenheimer, H.W. Rix, A. Borch, S. Dye, M. Kleinheinrich, L. Wisotzki and D. McIntosh, *Nearly 5000 distant early-type galaxies in COMBO-17: A red sequence and its evolution since* $z \sim 1$, Astrophys. J. **608** (2), 752-767, 2004.

[8] E. Chandler and S. Bate, *Inference for clustered data using the independence loglikelihood*, Biometrika **94** (1), 167-183, 2007.

[9] G. Chen and N. Balakrishnan, *A general purpose approximate goodness-of-fit test*, J. Qual. Technol. **27** (2), 154-161, 1995.

[10] B. Efron, *Logistic regression, survival analysis, and the kaplan-meier curve*, J. Amer. Statist. Assoc. **83** (402), 414-425, 1988.

[11] B. Emlet, R. McEdward and R. Strathmann, *Echinoderm larval ecology viewed from the egg*, Echinoderm Stud. **2**, 55-136, 1987.

[12] N. Eugene, C. Lee and F. Famoye, *Beta-normal distribution and its applications*, Comm. Statist. Theory Methods **31** (4), 497-512, 2002.

[13] F. Famoye, C. Lee and N. Eugene, *Beta-normal distribution: Bimodality properties and application*, J. Mod. Appl. Stat. Methods **3** (1), 85-103, 2004.

[14] H.W. Gómez, H.S. Salinas and H. Bolfarine, *Generalized skew-normal models: Properties and inference*, Statistics **40** (3), 495-505, 2006.

[15] W. Hardle, *Smoothing Techniques with Implementation in S*, Springer, 1991.

[16] M.Y. Hassan and R.H. Hijazi, *A bimodal exponential power distribution*, Pakistan J. Statist. **26** (2), 379-396, 2010.

[17] P.V.S. Sarma, K.S. Rao and R.P. Rao, *On a family of bimodal distribution*, Sankhya A **52** (3), 287-292, 1990.

[18] C.E. Shannon, *A mathematical theory of communication*, Bell Syst. Tech. J. **27**, 379-432, 1948.

[19] O. Venegas, H.S. Salinas, D.I. Gallardo, H. Bolfarine and H.W. Gómez, *Bimodality based on the generalized skew-normal distribution*, J. Stat. Comput. Simul. **88** (1), 156-181, 2018.

[20] N.A. Weber, *Dimorphism in the african oecophylla worker Nd an anomaly (hym.: Formicidae)*, Ann. Entomol. Soc. **39** (1), 7-10, 1946.

[21] S. Weisberg, *Applied Linear Regression*, Wiley and Sons, Inc., 2005.

[22] E.O. Wilson and R.W. Taylor, *A fossil ant colony: New evidence of social antiquity*, Psyche (Camb Mass) **71** (2), 93-103, 1964.

[23] K. Xu, M. Xie, L.C. Tang and S.L. Ho, *Application of neural networks in forecasting engine systems reliability*, Appl. Soft Comput. **2** (4), 255-268, 2003.